Accepted Manuscript

Title: High-content analysis for drug delivery and nanoparticle applications

Author: id="aut0005" biographyid="vt0005" orcid="0000-0002-8781-8344"> David J. Brayden Sally-Ann Cryan Kenneth A. Dawson Peter J. O'Brien Jeremy C. Simpson

PII: S1359-6446(15)00145-2
DOI: http://dx.doi.org/doi:10.1016/j.drudis.2015.04.001
Reference: DRUDIS 1607

To appear in:

Received date: 18-12-2014
Revised date: 9-3-2015
Accepted date: 13-4-2015

Please cite this article as: Brayden, D.J., Cryan, S.-A., Dawson, K.A., O'Brien, P.J., Simpson, J.C.,High-content analysis for drug delivery and nanoparticle applications, *Drug Discovery Today* (2015), http://dx.doi.org/10.1016/j.drudis.2015.04.001

Highlights

• High content analysis (HCA) gives fluorescent imaging data on cell parameters in live cells

• HCA is now used in to monitor sub-lethal cellular toxicology of drug delivery vehicles

• Data on permeation enhancers, polymers and nanoparticles is reviewed

• The data yields quantitative detailed information from up to 72 hour cell exposures

• HCA also tracks nanoparticle intracellular routing in cells and siRNA can dissect pathways

High-content analysis for drug delivery and nanoparticle applications

David J. Brayden[1,3], Sally-Ann Cryan[3,4] , Kenneth A. Dawson[5], Peter J. O'Brien[1], and Jeremy C. Simpson[6]

[1]University College Dublin (UCD) School of Veterinary Medicine, Dublin 2, Ireland
[2]UCD Conway Institute, Dublin 2, Ireland[LM1]
[3]School of Pharmacy, Royal College of Surgeons in Ireland, Dublin 2, Ireland
[4]Trinity Centre for Bioengineering, Trinity College Dublin, Dublin 2, Ireland
[5]UCD Centre for Bionano Interactions, School of Chemistry and Chemical Biology, Belfield, Dublin 4, Ireland
[6]UCD School of Biology and Environmental Sciences, Belfield, Dublin 4, Ireland
[LM2]*Keywords:* high content analysis; high content screening; nanoparticle uptake; polymer toxicology; sub-lethal cellular toxicology; intracellular nanoparticle pathways.
Corresponding author: Brayden, D.J. (David.Brayden@ucd.ie)
Teaser: High-content analysis is being adapted to examine nanoparticle trafficking in cells and to assess the sublethal mechanistic effects of polymers, excipients, and permeation enhancers.

Author biographies

David J. Brayden
David Brayden is a pharmacologist and professor of advanced drug delivery at University College Dublin (UCD), Ireland. From 1991 to 2001, Brayden was a senior scientist at Elan Biotechnology Research specializing in oral peptide transport. From 2007 to 2013, he was director of the Science Foundation Ireland (SFI) Strategic Research Cluster, the Irish Drug Delivery Network. He is current deputy coordinator of a European Union (EU) FP7 consortium working on oral nanomedicines (TRANS-INT) and a principle investigator in the new SFI Centre for Medical Devices (CURAM). His main research is in oral peptides and drug–device combinations.

Sally-Ann Cryan
Sally-Ann Cryan has a pharmacy degree and a PhD in pharmaceutics (2002) from Trinity College Dublin. She was awarded the US Fulbright Scholarship in Science and Technology in 2002 and returned as a lecturer to the Royal College of Surgeons in Ireland (RCSI) in 2004. She is currently associate professor of pharmaceutics and pharmacy research lead within the School of Pharmacy, RCSI. She is also a principle investigator in the Tissue Engineering Research Group in RCSI and the Trinity Centre for Bioengineering. Her main research is in pulmonary delivery of nanoparticles.

Jeremy Simpson
Jeremy Simpson carried out his PhD at the University of Warwick, followed postdoctoral work at the Scripps Research Institute in San Diego, and the Imperial Cancer Research Fund in London. After 9 years as a staff member at the European Molecular Biology Laboratory (EMBL) in Heidelberg (Germany), he was appointed as professor of cell biology at UCD, in 2008. He currently applies high-throughput imaging technologies to study subcellular transport pathways and the internalization routes taken by nanoparticles in cells. He runs the UCD Cell Screening Laboratory and is the author of more than 80 publications.

High-content analysis (HCA) provides quantitative multiparametric cellular fluorescence data. From its origins in discovery toxicology, it is now addressing fundamental questions in drug delivery. Nanoparticles (NPs), polymers, and intestinal permeation enhancers are being harnessed in drug delivery systems to modulate plasma membrane properties and the intracellular environment. Identifying comparative mechanistic cytotoxicity on sublethal events is crucial to expedite the development of such systems. NP uptake and intracellular routing pathways are also being dissected using chemical and genetic perturbations, with the potential to assess the intracellular fate of targeted and untargeted particles *in vitro*. As we discuss here, HCA is set to make a major impact in preclinical delivery research by elucidating the intracellular pathways of NPs and the *in vitro* mechanistic-based toxicology of formulation constituents.

A brief recap of cytotoxicity assays
In vitro cell-based assays have long been used to assess the cytotoxic effects of drug exposure [1]. Cells undergoing acute necrosis swell and lose metabolic capacity, thereby losing the capacity to maintain a barrier to the extracellular space and the ability to reproduce. Initial assays measured cell counts and morphological changes associated with cell death. Effects were detected by assessment of the maintenance of plasma membrane integrity, as reflected by exclusion of dyes, including trypan blue, eosin, propidium iodide (PI), or crystal violet [2]. The

corollary was the failure of live cells to internalize supravital dyes, including neutral red, into lysosomes [3]. Therefore, by dual staining with trypan blue and neutral red, live and dead cells could be counted microscopically. Incorporation of [^{3}H]-thymidine or 5-bromo-2-deoxyuridine into newly synthesized DNA became a common indicator of cell proliferation in immunological and oncology studies, respectively [4]. Leakage of lactate dehydrogenase (LDH) or potassium ions had an advantage of being more sensitive than dye exclusion or cell growth assays, because the latter are ineffective in acute toxicity studies as a result of insufficient proliferation during acute exposure. Trypan blue exclusion is an insensitive indicator of loss of cell viability, changing much later than LDH release, which in turn is less sensitive than the release of potassium and influx of sodium. This difference is likely to be attributable to the smaller size of an ion versus that of a large enzyme. Release of [^{51}Cr] from prelabeled cells became a common assay for the quantitation of cell-mediated cytotoxicity [5], although LDH release was more convenient, precise, and less expensive [6]. Many of the post-1980 assays focused on measuring the loss of reductive activity using dyes that were reduced in proportion to the activity of electron transport. Such assays are run on high-throughput, colorimetric or fluorescence-intensity, microtiter-plate readers, but crucially lack the ability to provide single cell resolution data. Thus, 3-(4, 5-dimethylthiazol-2-yl)-2,5-diphenyltetrazolium bromide (MTT) was reduced by NADH generated by cell metabolism to a purple formazan precipitate, which reflects cytotoxicity, proliferation, or cell activation [7]. Other tetrazolium salts that yield a soluble formazan followed, along with the introduction of intermediary electron acceptors, such as phenazine methosulfate, to facilitate dye reduction [8]. The sensitivity of dye approaches was increased with a halving of assay time and reduction of costs by introduction of the Alamar Blue assay [9], which had a good correlation with neutral red uptake, LDH release, total protein, and cell density [10].

Other viability assays were developed that monitored changes in intracellular activity. Rhodamine-123 was the first mitochondrial membrane potential dye to become available and provided an earlier indicator of the loss of cell viability compared with trypan blue [11]. Relatively nontoxic, fluorescent dyes for the quantitation of intracellular ionized calcium were discovered and used to assess viability [12]. Given that there is a 10 000-fold gradient in free calcium concentration across the plasma membrane, a prolonged rise in intracellular calcium concentration indicates impaired cell health. For example, nonspecific membrane-perturbing agents, such as halothane, produce concentration-related increases in cytosolic calcium [13]. Many assays focus on the measurement of cell mass, which increases with cell growth and proliferation, but decreases with cytotoxicity. This effect can be quantified by fluorescent microtiter-based measurements of total DNA [14], total protein [15], or ATP content [16]. These and the reductive dye assays have greater throughput and ease of performance compared with the [^{3}H]-thymidine incorporation. Several cytotoxicity assays have been specifically developed for the assessment of apoptosis, including detection of plasma membrane annexin V, caspase activation, and shrinkage and fragmentation of nuclei. The implementation of sophisticated assays for screening during the 1990s resulted from the development and automation of multiwell, microtiter-plate high-content readers and the development of relatively nontoxic, subcellular, fluorescent dyes [17]. These sensitive assays screen overt and acute cytotoxicity and have a major role in drug discovery [13].

In vitro cytotoxicity and predicting drug attrition

A 7-year, international, multicenter study (MEIC) involving 29 laboratories and 61 different cytotoxicity assays evaluated the relevance of *in vitro* cytotoxicity testing in numerous cell types in relation to *in vivo* human toxicity [18]. Fifty chemicals were studied, including poisons, prescription drugs, substances of abuse, and common household chemicals. The *in vitro* cytotoxic concentrations were compared with known, acutely lethal doses in humans and showed predictive correlations of up to 88% [19]. The MEIC study suggested that assays with human cell lines give the best prediction and are independent of cell type, thereby indicating that the mechanism of toxicity was inhibition of a common, vital cell process. Other studies also provide further convincing evidence that *in vitro* cytotoxicity assays are highly predictive of acute human drug toxicity [20,21].

A retrospective study of concordance of human toxicity for 150 drug candidates in clinical trials was established and demonstrated close correlation with regulatory animal studies [22]. Human toxicity concordance was 71% for both rodent and nonrodent species, 63% for nonrodents alone, and 43% for rodents alone. Toxicity was identified in studies of duration of 1 month or less for 94% of toxicities. Concordance of animal and human toxicity varied depending on the type of toxicity: 91% (hematologic), 85% (gastrointestinal), 80% (cardiovascular), but only 37% (cutaneous hypersensitivity) and 55% (hepatic) for others. Even though prediction from preclinical animal models is especially low for human hepatotoxicity and cutaneous toxicity, when these occur, the candidate is likely to be terminated in clinical development despite the risk of a false positive. Although there is predictive value of regulatory animal studies for many human toxicities, drug safety remains an important cause of marketplace attrition. Of drug candidates entering clinical development from 2006 to 2010, ~25% failed because of safety issues [23]. Recognition of the high impact of safety-related attrition of drugs throughout all phases of discovery and development drove the implementation of novel cytotoxicity screens early in discovery to identify overt and acute toxicity [13]. Therefore, conventional cytotoxicity assays have been incorporated into drug discovery screening strategies because they use similar cell types, culture methods, and monitoring and measuring technologies as the other cell-based assays used to screen for appropriate efficacy or bioavailability. Additionally, preclinical development safety strategies typically include specific cytotoxicity assays for genetic toxicity using the *in vitro* micronuclei assay [24], and also when knowledge of the compound chemistry indicates specific risks, such as for

phototoxicity using the neutral red uptake assay in 3T3 fibroblasts [25]. Unfortunately, these conventional screens have deficiencies in sensitivity and selectively, which impact the quality of prediction.

The HCA track record in drug discovery

The advent of HCA use in drug discovery *in vitro* toxicology over the past decade was an important departure in that it provide multiparametric mechanistic data in live cells in real time and this meant that, although animal toxicology was still needed to support first-in-man trials, there was greater confidence in achieving predictive outcomes with fewer false positives and false negatives. A cell-based HCA model demonstrated an order-of-magnitude increase in the concordance of *in vitro* cytotoxicity with human toxicity as part of an analysis of 250 marketed drugs over conventional cytotoxicity assays [26]. It focused in particular on low-incidence idiosyncratic hepatotoxicity. Since then, HCA has been widely introduced into safety programmes in drug discovery [27–30]. Its effectiveness in identifying cytotoxicity has now been extended from small molecules to biotech molecules, NPs, polymers, and intestinal permeation enhancers. Applicability is across a range of cell types, including hepatic, intestinal, renal, skeletal and cardiac myocytic, neuronal, lymphocytic, and monocytic [31]. In addition, its effectiveness at identifying specific subcellular toxicities has been improved by the incorporation of fluorescent dyes that detect genetic, mitochondrial, lysosomal, and oxidative stress-associated effects. One of the first examples of a HCA cytotoxicity assay in discovery was the generation of 12-point concentration–response curves for drug-induced cytotoxic changes during 3-day exposures of HepG2 hepatocytes [26]. Up to seven drugs and controls were tested per 96-well plate. The cytotoxic changes monitored were mitochondrial membrane potential using tetra-methyl rhodamine (TMRM), intracellular ionized calcium using Fluo-4, surface membrane permeability to small molecules using Toto-3, and cell proliferation and nuclear area using Hoechst-33258. A typical work plan is outlined in Figure 1. A HCA example of the cytotoxic effects of fluvastatin and mitoxantrone in HepG2 and Jurkat lymphocytes, respectively, over a 72-h exposure is shown in Figure 2 (P.J. O'Brien, unpublished data, XXXX[LM3]). Concentration–response curves were horizontal for nontoxic compounds, but had an inflection upwards or downwards beyond background for cytotoxic molecules. The concentration at which deflection occurred was defined as the cytotoxic concentration and the interpretation of significance depends on normalizing these values to the maximum efficacious blood concentration (Cmax), thereby generating a therapeutic index (TI) (cytotoxic concentration/Cmax). Drugs for which this value exceeds 100 are considered safe with 90% confidence. In a head-to-head comparison of the HCA with conventional cytotoxicity assays, concordance with human toxicity was assessed. The HCA assays had almost 95% specificity, with few false positives. However, whereas false negatives typically exceeded 80% for conventional assays, they were less than 10% for HCA [26]. Frequently, cytotoxicities were found using HCA for drugs without known human hepatotoxicity potential. These could be attributed to the cytotoxic effect that they had in other human target organs, such as cardiotoxicity, nephrotoxicity, or neurotoxicity. Thus, HCA in hepatocytes identified not only human hepatotoxicity potential, but also toxicity potential for other organs. Therefore, HCA can be summed up as a combination and computerized automation of: (i) epifluorescence microscopy within an environmental chamber to maintain viability while monitoring cells; (ii) multifluorescence-intensity microtiter-plate reading to collect the data with high content, sensitivity, and speed; and (iii) software for object segmentation and analysis.

There are several features of the HCA model that distinguish it from regular cytotoxicity assays (Table 1). First, single cell microscopic imaging enables subcellular, spatial resolution to the precise level at which pathology and signal generation correlate with cytotoxicity. The state of apoptosis can be measured by examining changes in the nucleus; oxidative stress is detected in the cytoplasm; cell integrity is assessed by plasma membrane potential changes; energy production is measured in mitochondria; and autophagy and accumulation of waste products or foreign material are features of lysosomes. The sensitivity, specificity, and resolution of measurement increase the precision and accuracy and reduce artifacts arising from extracellular fluorescence, dead cells, or cells of another origin. Such cells can be automatically excluded from the analysis using definable and measureable features. HCA imaging enables the full diversity and asynchronicity of individual cellular changes to be seen, which are typically summated in conventional population-based assays. For example, proliferation can be decreased overall, but some cells can also undergo an adaptive increase in a signal, thereby cancelling out a decrease in another cell because of its loss of viability [32]. A second advantage of HCA is multiparametric monitoring. Until the introduction of HCA, no more than two fluorescence signals could be monitored simultaneously. With HCA, not only can the intensities and kinetics of four separate fluorescent signals of intracellular activities be monitored simultaneously, but the subcellular structures from which they originate can also be morphometrically analyzed. This yields information on changes in the number, shape, and size of individual cells, and their nuclei and other membrane organelles. Third, HCA cytotoxicity enables live cell measurements of structural, functional, and biochemical parameters in an environmental chamber in which gaseous composition, temperature, and humidity have been optimized for cell viability. This minimizes environmentally induced changes that could confound chemical-induced effects on cells and is often a feature on nonHCA assays. Recently, it was confirmed that, unless plate humidity is well controlled in HCA, an 'edge effect' can occur in which evaporation occurs more at the outer wells and in corner wells and can cause erroneous interpretation of drug effects [33]. Fourth, many cytotoxic events only become apparent at later assay time points, so 72-h drug exposure to pre-acclimatized cells is needed and this is not typical in conventional assays. Fifth, the high content of information that is obtained is achieved at a relatively high throughput compared with conventional assays. The advantage of this is the increased user-friendliness and decreased instrument

operator-time required for HCA. Interassay variability is reduced, because more samples can be run. Finally, HCA has capacity for the inclusion of increased points for more precise definition of concentration–response curves, and also the inclusion of additional positive and negative controls.

However, there are several limitations to HCA. First, if the cytotoxicity is pharmacologically mediated via a specific receptor associated with a cell type, then it may not manifest. Second, many hepatoxicities result from toxic metabolites arising via cytochrome P-450. Thus, if the selected line does not have appropriate xenobiotic metabolic capacity, it will generate false negatives. Fortunately, during the 72-h exposure of HepG2 hepatocytes to drugs, metabolic competence develops. Third, most drugs are toxic if they are sufficiently bioavailable and the dose is high enough *in vivo*; therefore, the significance of a cytotoxic HCA finding requires a TI calculation to enable the HCA data to have predictive value.

HCA: cytotoxicity of polymers and permeation enhancers

From its pioneering use in toxicity screening in drug discovery, HCA is now supporting comprehensive toxicity screening in drug delivery, NP, and biomaterial applications. Materials used to date in drug delivery applications have been assessed for *in vitro* toxicity by standard *in vitro* viability assays with heavy reliance on expensive preclinical toxicology packages, especially in rodents and dogs, and, to a lesser extent, in cynomolgus monkeys. In addition, for regulatory reasons, the industry has tended to be conservative in opting for materials for delivery applications that have excipient status or a long history of use in humans, whereas academic groups are less constrained. The potential cytotoxicity of gene delivery vectors, including cationic polymers, dendrimers, and polyethyleneimine (PEI), is a major concern because they have access to intracellular machinery and are liable to induce off-target effects. Rawlinson and colleagues [34] were the first group to use HCA to test the cytotoxicity of a mucoadhesive antibacterial polymer and potential gene delivery vector. Poly(2-(dimethylamino ethyl)methacrylate) (pDMAEMA) was tested on human Caco-2 intestinal epithelial cells and U937 monocytes. The authors compared the sublethal effects of pDMAEMA on seven parameters at different concentrations and exposure times, and then compared the data with histology of sections of rat intestinal mucosae exposed to high concentrations for 60 min. At extremely high *in vitro* concentrations for 72 h in both cell lines, pDMAEMA increased nuclear intensity and intracellular calcium, but decreased nuclear area, plasma membrane potential, mitochondrial membrane potential, and cell number, and did not cause phospholipidosis (Figure 3). EC_{50} values for parameter changes were lower than those seen by MTT assay, thus providing evidence that such events preceded and ultimately contributed to necrosis and cell death; however, these changes were largely irrelevant at high concentrations that are unlikely to be encountered *in vivo*. As a confirmation of the innocuous nature of pDMAEMA predicted by HCA, it did not induce any histological damage on isolated rat colonic mucosae and caused on only mild damage to ileal tissue at even higher concentrations of the agent, with exposure for a more realistic 120 min compared to 72 h with cell lines. Therefore, the data supported the potential use of pDMAEMA as a gene delivery agent [35] and as an antibacterial surface coating [36], with some confidence in the likelihood of a safe outcome from a full preclinical toxicology package. HCA has also been used to study the mechanisms of cytotoxicity for two of the most common cationic polymeric carriers, PEI and poly-L-lysine (PLL) [37]. These agents induce significant *in vitro* cytotoxicity, but the mechanisms are not well understood. Real-time high-content imaging was used to monitor polymer-induced cytotoxicity in HepG2 cells in assessing cytosolic calcium, caspase 3, and mitochondrial membrane disruption. Interesting differences between the two polymers were found, with PEI inducing apoptosis via an intrinsic pathway, whereas PLL did so via both the intrinsic and extrinsic caspase cascade. The molecular weight of both polymers, as well as the PEI structure (branched or linear), had a significant effect on apoptotic activity.

In oral drug delivery, there is considerable debate on the safe and effective use of intestinal permeation enhancers (PEs) to deliver poorly absorbed peptides, proteins, and macromolecules. Peptides, including insulin, are unstable and poorly permeate the small intestinal epithelium, hence their low oral bioavailability [38]. PEs are present in several solid-dose oral formulations for peptides, of which two technologies are advanced clinically [39,40]. Examples of advanced PEs include medium-chain fatty acids (MCFAs), acyl carnitines, bile salts, and alkyl maltosides [41]. Major issues for potential oral peptide formulations include the commercial cost of losing the majority of payload, and the possible damage to the intestine that can give rise to inflammation as well as pathogen absorption following repeated administration in formulations containing PEs. Restrictions to the nomination of a suitable peptide candidate are that it must have a low molecular weight (<10 000 Da), be potent, and have a wide TI to be able to cope with the large intrasubject variation in plasma levels seen with low oral bioavailability. More effective enhancer candidates are being assessed, but the problem is that the TI of these agents tends to be narrow compared with many of the peptides that they are being matched with. One such PE candidate was a 26-amino acid cationic antimicrobial peptide, melittin, isolated from the venom of the honey bee, *Apis mellifera*. Melittin not only perturbs bacterial membranes, but is also hemolytic to mammalian erythrocytes at similar concentrations [42]. HCA on Caco-2 cells examined systematic amino acid replacement in melittin analogs to discover whether peptides with the best efficacy and lowest effect on cell cytotoxic parameters could be synthesized [43]. Reduced changes in plasma membrane potential and mitochondrial membrane potential were seen with analogs with lower hydrophobicity compared with the parent melittin molecule, but unfortunately this also led to a reduction in transcellular permeation enhancement. Importantly, the IC_{50} values for the cell parameters were lower than those obtained in the MTT and rat erythrocyte hemolytic assays, suggesting that these cellular changes ultimately brought about cell death. Although these data suggested that melittin and its analogs cannot be further developed

as oral PEs *per se*, prodrug modifications have recently enabled melittin to be used as part of a successful gene delivery construct when grafted onto *N*-(2-hydroxypropyl)methacrylamide (HPMA) and pyridyl disulfide methacrylamide (PDSMA) block copolymers, following intracerebral injection to mouse brain [44]. Elsewhere, formulation of melittin in the lipid membrane of a perfluorocarbon NP reduced systemic toxicity and permitted localization in mouse tumour cells [45]. Thus, HCA confirmed the nonspecific cytotoxic actions of melittin and this has led to elegant constructs that have potential in both nonviral gene delivery and anticancer applications. HCA also similarly defined the polyketide mycotoxin, patulin, as an intestinal PE whose membrane effects could not be dissociated from cytotoxicity on Caco-2 cells and this led to abandonment [46].

Therefore, HCA has been useful in deciphering the mechanism of action of delivery agents and confirming some of them to be toxic, and in establishing the innocuous nature of others. In addition, it has also provided rank-order data on the parameters for the sodium salts of a range of MCFAs [33], several of which are key components of oral delivery formulations for poorly absorbed molecules. By correlating Caco-2 cell changes in HCA parameters for the C_8–C_{12} MCFAs with hydrophobicity, critical micellar concentration and efficacy as permeation enhancers across Caco-2 monolayers, a pattern emerged showing that the best enhancers (C_{11} and C_{12}) were the most hydrophobic and had the lowest critical micelle concentrations; however, these dramatically perturbed the plasma membranes and were the most cytotoxic (Figure 4, Table 1). These data supported the inclusion of C_8 and C_{10} in the most clinically advanced oral peptide formulations: although they are not necessarily the most effective MCFAs as PEs, they are likely to be safer than C_{11} and C_{12}.

HCA has also been used to dissect damage–repair cycles in Caco-2 cells and filter-grown monolayers exposed to C_{10}. Although it is well known that the instilled rat intestinal mucosa is restituted within 45 min in response to exposure to surfactants, including SDS [47] and C_{10} [48], investigations of Caco-2 monolayer recovery have not gone much beyond noting the restoration of basal levels of transepithelial electrical resistance (TEER) in fresh medium, a process that can take up to 24 h (e.g., [49]). However, HCA revealed that, when Caco-2 cells were exposed to 8.5mM C_{10} for 60 min, nuclear intensity, intracellular calcium, nuclear area, plasma membrane potential, mitochondrial membrane potential, and cell number were all increased [33]. However, upon re-incubation in fresh media, all parameters reverted to normal levels within 60 min. Higher concentrations of C_{10} and longer exposure times were required to cause cell death as determined by the MTT assay [33]; therefore, these data reflect reversible sublethal effects that yield valuable insight into the mechanism of action. Importantly, 8.5-mM C_{10} is the same concentration that increased *in vitro* fluxes across monolayers. More than tenfold higher concentrations of 100-mM C_{10} are used in solid dose oral peptide formulations *in vivo* [50], well above the CMC [LM4]of 13–26 mM, so at least part of the action when presented as oral tablets for human trials is likely to be the result of surfactant-based perturbation of intestinal epithelial membranes. When intestinal dilution and transit time are factored in, it is still likely that tight junction openings are also induced at the lower C_{10} concentrations that might arrive at the epithelial wall. Overall, the data support a mechanism of action in which there is a combined action on increasing permeation via both paracellular and transcellular routes, but the relation between them is complex.

Further studies examining membrane perturbation effects of C_{12} on undifferentiated Caco-2 cells revealed that several agents, including taurine and L-glutamine, are cytoprotective through activation of calcium-ATPases in the plasma membrane as well as via increased mitochondrial calcium buffering and reduced mitochondrial cytochrome C leakage [51,52]. Related to this, pre-exposure to the prostaglandin E1 (PGE_1) agonist, misoprostol, also prevented C_{10}-induced increases in the apparent permeability coefficient (Papp) of mannitol and associated TEER reductions across Caco-2 monolayers, isolated rat colonic mucosae, and in rat colonic instillations *in vivo*; these data were correlated with a reversal of HCA parameter changes induced by C_{10} [53]. Therefore, HCA deciphered the mechanism in Caco-2 cells and monolayers through which C_{10}-induced increases in intracellular calcium, plasma membrane potential, and mitochondrial membrane potential; these effects were prevented by pre-incubation with 10-nM misoprostol in part via the prostanoid EP1 receptor. The data provided evidence of a membrane-stabilizing effect of misoprostol and confirmed actions of C_{10} on the plasma membrane. Petersen *et al*. [54] also used HCA with the oral permeation enhancer, tetradecyl maltoside (TDM), and confirmed that its weak effects on parameters in Caco-2 cells were in line with those expected of a mild non-ionic surfactant; these data were closely matched with largely innocuous histological effects on rat intestinal mucosae.

HCA: cytotoxicity of NPs

NP research is a major component of drug delivery science, because it aims to facilitate reduction in toxicity and improvement in pharmacokinetics of established injectable products, especially anticancer agents [55]. It is also an important strategy in attempts to negotiate the blood–brain barrier (BBB) to treat central nervous system (CNS) disease [56], as well as for the oral delivery of poorly permeable molecules, including peptides and proteins [57]. There appears to be clinical potential for systemically injected targeted NPs using ligands designed to bind receptors overexpressed on cancer cells or on the BBB [58,59], but there is a recognition issue caused by opsonin-based coronas depositing on the surfaces of targeted NPs in the circulation [60]. There is also a growing focus on local targeted delivery of NPs to disease sites that would overcome some of these issues for specific therapeutic needs, such as nebulization to the respiratory tract [61] and implantation within tissue engineering scaffolds [62], Therefore, with myriad organic and inorganic NP constructs emerging, it is important to systematically compare the cytotoxicity of families of (untargeted) NPs to examine the mechanistic basis of lethal and sublethal events in specific cell types following acute and chronic exposure. Along with the material itself, small changes in the

formulation process, particle diameter, zeta potential, surface coating, duration of exposure, and particle stability can impact plasma membrane binding, intracellular accumulation, and cytotoxic parameters. It has been pointed out that NPs with apparently low toxicity might still produce sublethal effects and that mechanistic studies require low concentrations at a range of exposure times [63], hence the need for HCA. Furthermore, there is evidence that NP formats of some agents, including inorganic metals, are more toxic compared with soluble formats [63], and this has contributed to the interest in developing appropriate predictive assays. Materials including polystyrene and other polymers tend to have low intrinsic fluorescence, whereas some metal particles and quantum dots (Qdots) can fluoresce; these tend to be in a defined excitation and emission window and have been well characterized. A fluorophore would need to be located in an excitation–emission window that is different from that defined for such particles. The modern fluorophores that are typically used in HCA applications (e.g., the Cy and Alexa dyes) are so bright that any intrinsic fluorescence from the material is inconsequential for imaging. One of the first HCA studies in this area examined the effects of 10-nm diameter polyethylene glycol (PEG)-coated silane semiconductor Qdots on human lung and skin fibroblast cell lines [64]. No changes in cell cycle parameters or evidence of apoptosis or necrosis were seen in lung cells at 8 and 80 nM over 24 h, and only a slight increase in the latter parameters was detected in skin fibroblasts. Along with data showing that these PEG-coated Qdots did not activate genes associated with inflammation, immunity, or heavy metal-based toxicity, this study revealed the low toxicity potential of surface-functionalized Qdots compared with the well-known toxicity of uncoated cadmium-releasing control Qdot formats.

In a related study, HCA was used to assess the cytotoxicity of two types of cadmium telluride (CdTe) Qdot on NG108-15 neuroblastoma cells [65]. One construct was thioglycolic acid (TGA) capped and the other was similarly synthesized, but used gelatin as a protective agent instead of PEG. The gelatin-based Qdots had a dramatically reduced effect on lowering cell count over 24 h compared with TGA-Qdots in undifferentiated cells. Moreover, the sublethal concentration of gelatin-based Qdots was four times lower than that of TGA-capped Qdots. Effects on mitochondrial membrane potential and cell calcium revealed that the gelatin-based Qdots caused less-significant changes compared with the TGA-based ones in the more-sensitive differentiated NG108015 cells. Moreover, these data were confirmed by measuring effects on neurite outgrowth, where the gelatin-based Qdots were less toxic than their TGA-capped counterparts at a concentration of 50 nm over 6 h. In the same study, the authors also examined gold (Au)-NP exposure to HepG2 human hepatocellular carcinoma cells for up to 6 h. Changes in cell count, nuclear area, mitochondrial membrane potential, and intracellular calcium were within 10% of control values and each was reversible in fresh medium. The most notable change was some inhibition of cell proliferation and intracellular calcium release. Reversibility of Au-NP induced cytoskeletal disruption of dermal fibroblasts has also been confirmed [66]. Still, potential toxicity of Au-NP remains a topic of debate because, although Au has been used as an antirheumatoid arthritis therapeutic for decades and is widely thought to have minimal toxicology, it now features in NP formats being developed for oral insulin [67] and injectable targeted anticancer payloads [68]. Size, shape, and functionalization might alter *in vivo* biodistribution and this has toxicity implications even for well-established materials [69].

From the above discussion, the selection of cell type and the state of cell differentiation are crucial decisions in HCA study designs. NP toxicology studies for systemic delivery applications require HepG2 cells, whereas human lung and skin fibroblast cell lines are more appropriate for aerosols and skin exposure, respectively. Other studies examining the biocompatibility of gelatin-based Qdots used human THP-1 macrophages, where reduced apoptosis was revealed compared with TGA-capped Qdots [70]. HCA has recently been applied to NP constructs derived from biomaterials using primary human fibroblast cultures [71]. Using lipid-based cationic NPs in a multiparametric assay, the authors proved that the basis of the reversible cytotoxic attack for an 8-h exposure was at the level of mitochondrial disruption, data that tallied with a capacity to activate Toll-like receptor 4 on monocytes and macrophages, leading to Type 1 cytokine release [72]. Elucidating such a specific mechanism of sublethal toxicity occurring at concentrations below those that induce cell death enables high-throughput screening for new lipid materials for NPs that can be designed to avoid altering mitochondrial parameters. As a final example, 50-nm aminated polystyrene NPs are well known to cause *in vitro* cytotoxicity. In one of the most complex NP studies with HCA in a high-throughput format to date, the fluorophore and parameter set up described in [26] was used to study the mechanistic aspects of how aminated NPs cause cytotoxicity compared with inert carboxylated NPs in seven cell lines originated from multiple tissues [73]. In most cell lines, there were similar IC_{50} values obtained for the aminated NPs, beginning with lysosomal acidification induced at low concentrations, followed by mitochondrial depolarization, nuclear condensation, cytosolic calcium increases, and plasma membrane potential. Data from two of the lines are illustrated in Figure 5. Furthermore, there was evidence of NP-induced phospholipidosis and steatosis that were associated with acidification of lysosomes.

HCA: particulate delivery to access intracellular targets

Optimal design for next-generation drug delivery vehicles will be informed by a greater understanding of how they interact with cells and the intracellular environment. Flow cytometry enables relatively high sample throughput and provides quantitative information with respect to the concentrations of NPs inside cells. However, it has become increasingly clear that the internalization and trafficking pathways taken by NPs are far from uniform and depend on a variety of factors, including the particle size, shape, material, and the surrounding corona [74]. Although flow cytometry might provide sufficient time resolution to study NP uptake and trafficking, it provides

relatively little spatial resolution. The precise intracellular environment that NPs pass through is essential for the design of drug carriers that can avoid acidic degradation in lysosomes [75]. Consequently, an increasing number of flow cytometry NP studies are now supported by quantitative fluorescence microscopy, particularly HCA.

With a desire to find alternative approaches to viral vectors because of safety, scale-up, and payload loading issues, a range of nonviral NPs have been explored over the past two decades for the delivery of plasmid DNA, small interfering (si)RNA and miRNA. Many have been based on polymeric carriers (e.g., PEI and PLL). The lack of well-defined criteria used for testing NP–cell interactions in the literature makes formulation comparisons difficult. Recent reports have identified how HCA could provide a potential solution to this problem by enabling libraries of NPs to be screened in parallel for specific biomedical applications, resulting in the rapid identification of lead delivery systems. For example, HCA was used to screen a library of 70 peptide-based gene delivery vectors for the delivery of plasmid (p)DNA into COS-7 cells [76]. These parameters included cytotoxicity and transfection efficiency in nondividing cells. The authors compared vector transfection efficiencies in delivering enhanced GFP plasmids (EGFP), whereas HCA enabled transgene expression at a single cell level across the entire cell population to be determined. The combination of robotics integrated with automated image acquisition and analysis decreased the analysis time and facilitated true high-throughput screening. Data from different studies had already shown that the 70 vectors could transfect multiple cell types, but complicating factors included a range of different incubation times and the presence or absence of serum, making head-to-head comparisons impossible. Therefore, HCA assessment [76] enabled standardization of the protocol for transfection in a single cell type in serum-containing medium over a 4-h incubation, followed by expression analysis after 48 h, thereby enabling rapid, reliable, comprehensive comparisons of the 70 peptides. Of note was that only five out of 70 peptides had high levels of transfection efficiency and it seemed that weak transfection capacity for the majority related to the presence of serum, which is often not included in transfection media *in vitro*, but which is highly relevant *in vivo*. Thus, HCA is a valuable *in vitro* tool capable of accelerating the development of transfection agents.

Similar to other nucleic acid based therapies, miRNA (endogenous small RNAs that act on mRNA at a post-transcriptional level and usually negatively regulate gene expression) technology is moving towards clinical evaluation, but delivery issues are a key impediment [77]. HCA can also assist in rank-ordering polymeric carriers for their capacity to deliver miRNA mimics (pre-miR) to cystic fibrotic (CF) airway epithelial cells and subsequently to modulate aberrant cystic fibrosis transmembrane conductance regulator (CFTR) expression [78]. There is a growing understanding that altered expression of miRNA is involved in the CF phenotype and, therefore, modulation of miRNA using pre-miRs presents a potential new therapeutic modality for CF. Fluorescently labeled miRNA was loaded into either PEI or chitosan-based NPs, which were then incubated with CF epithelial cells on a 96-well plate and, following a 20-h incubation, the cells were washed, fixed, and stained with phalloidin-fluorescein isothiocyanate (FITC) for F-action, and with Hoechst 33342 for the nucleus, followed by HCA. The level of miRNA associated with the CFBE41o- cells was polymer dependent, with PEI facilitating significantly more association compared with chitosan (Figure 6). Subsequently, miR-126 [an miRNA that modulates Target of Myb protein 1 (TOM1) expression] was encapsulated in PEI constructs and the assay reflected significant modulation of TOM1 expression with a range of PEI-miRNA with different nitrogen:phosphate (N:P) ratios. Of the formulations tested, PEI-miRNA with a ratio of N:P 1:1 effected the greatest TOM1 knockdown, but they were not the most effective in terms of either particle–cell association (by HCA), or in pre-miR-126 delivery (by qRT-PCR). Therefore, HCA appears to be useful in the initial screening of miRNA-NP cell uptake, but downstream functional assays are ultimately required to determine efficacy.

HCA is also being used to compare polymeric microparticle (MP)-based systems. Poly (lactic-co-glycolic acid) (PLG) microparticles were prepared in a range of sizes (0.8–24 Mm) to determine the most effective size for uptake by alveolar macrophages (AM) [79]. Macrophages internalize microparticles very effectively, but there is little systematic study of what the optimal size particle required to achieve internalization might be. The goal of this work was to develop a delivery platform for the targeted delivery of antitubercular agents to the site of *Mycobacterium tuberculosis* infection in AM. HCA data indicated an optimal size range of 0.8–2.1 Mm for PLGA MPs for macrophage uptake. However, spectrofluorimetry did not reveal significant discrimination, because of its inability to measure individual particles of a specific size per cell. CLSM, while providing detailed qualitative intracellular trafficking information, was also limited in terms of quantitative analysis of microparticle uptake because of the subjectivity involved in cell selection, counting errors, and the limited number of samples that can be analyzed. The information from HCA study has been used to harness PLG-based MPs for delivery of a range of therapeutic cargoes requiring intracellular delivery to macrophages, including short hairpin (sh)RNA, siRNA, and miRNA [80] (Figure 7). Thus, HCA offers a useful additional tool to discriminate accurately intracellular delivery of particles across a range of particle sizes.

Another key group of materials that have been extensively explored as particulate delivery systems are lipids. HCA was used to monitor lipid-based NPs loaded with traceable siRNAs in cell lines and in mouse liver cells i to quantify siRNA uptake and intracellular trafficking [81]. The lipid NPs comprised ionizable lipid/ distearoyl phosphatidyl choline/cholesterol/,PEG-DMG in ratios of 50:10:38.5:1.5 and entrapped antiGFP siRNA labeled with Alexa Fluor 647. The NPs entered cells by both constitutive and inducible pathways in a cell type-specific manner. HCA was done in two sequential rounds of calculations, first to identify the NPs and then their intracellular location. Particular focus was placed on the role of endosomal release on the pharmacokinetics of the NPs and this was studied using the early endosome markers, EEA1 and Rabankyrin-5, and the late endosome marker, LAMP1.

The authors determined the colocalization of the markers with the NPs over time. HCA allowed detailed quantitative analysis of the time-dependent colocalization of the NPs with the endolysosomal compartments. Escape of the siRNA from NPs was unexpectedly determined to be very low (1–2%), but the real impact lay in the harnessing of the instrumentation together with appropriate sample preparation to enable systematic study of the intracellular distribution of NPs. Others used high-throughout confocal microscopy to study the uptake and intracellular trafficking of siRNA-loaded lipid NPs, which were manufactured using microfluidics and included a cationic lipid (C12-200) [82]. The antiGFP siRNA-loaded NPs were used to transfect HeLa-GFP-expressing cells and several small molecule inhibitors were used that alter cell signaling and intracellular trafficking and that either inhibit or induce autophagy. Protein–protein and protein–small molecule interaction networks were then derived using a systems biology approach. siRNA was used to deplete key endocytotic regulators in the HeLa cells to identify internalization pathways used by the cationic lipid NPs, which were determined to be primarily by macropinocytosis. For a third lipid-based example of HCA application, a range of liposomes was recently screened for their capacity to deliver siRNA to macrophage-like cells [83]. Neutral, anionic, and mannose-coated liposomes were prepared in five sizes (100 nm, 200 nm, 400 nm, 1000 nm, and >1 mm), fluorescently labeled with phosphatidylethanolamine-rhodamine, and then analyzed for interaction with differentiated THP-1 cells, a macrophage model. In sum, 25 different liposome constructs were studied in parallel under the same conditions and, as a result, lead platforms were identified that had the most significant THP-1 cell association: anionic DOPS-based liposomes and mannose (MC6C)-coated liposomes.

A recent study used high-content imaging to study the effects of surface charge and surface hydrophobicity of Au-NPs on cell interactions [84]. Two-nm NPs with variable charge and hydrophobicity and a multiparametric methodology were used to study the interaction with human umbilical vein endothelial cells (HUVECs) and C17.2 neural progenitor cells. HCA and gene expression studies determined whether there was a correlation between the particle surface properties, membrane damage, and autophagy. The study found that, whereas higher levels of hydrophobicity induced autophagy and increased cell membrane damage, overall surface hydrophobicity did not substantially alter uptake of NPs into cells. Although these studies focused on characterizing specific delivery systems in detail, automated instrumentation provides an important new tool for materials science and drug delivery researchers to use to screen biocompatible particle delivery systems for intracellular targeting. These automated HCA systems are enabling nanomaterial structure–activity relations to be developed and are likely to aid future excipient and biomaterial discovery [85].

HCA: detailed mechanisms of NP internalization and intracellular trafficking

HCA has not yet been applied in a large-scale systematic way to dissect NP internalization and trafficking, although several single cell quantitative microscopy-based studies (i.e., low-throughput HCA) have been carried out. Quantification has typically relied on measuring the fluorescence intensity of intracellular NPs. One of the first studies to reconcile imaging with quantitative flow cytometry data analyzed latex beads of diameters of 50–1000 nm in nonphagocytic mouse melanoma cells. Chemical perturbations of the clathrin- and caveolin-dependent endocytic pathways revealed that, for this particle type, clathrin-mediated endocytosis was predominant for particles <200 nm, whereas above this nominal size, caveolin-dependent machinery was predominant [86]. However, particle composition is also influential, because similar flow cytometry and imaging studies using PLL-g-PEG DNA-complexed particles of 80–90 nm revealed that inhibition of clathrin-mediated uptake with chlorpromazine did not reduce internalization into COS-7 cells [87]. Although, genistein (an established inhibitor of caveolin-mediated uptake) reduced the uptake of these particles, the kinetics of internalization and the lack of colocalization with caveolin suggested that multiple machineries effect uptake of this particle type. A more recent study across a wider range of cell types further endorsed this thesis for PEG-based particles [88].

Surface charge on particles is another key determinant for the uptake mechanism used. Using 100-nm polystyrene NP, spinning disk microscopy and quantitative image analysis were used in mesenchymal stem cells to show that carboxylated-functionalized polystyrene NPs were internalized fivefold more efficiently than nonfunctionalized anionic NPs [89]. More interesting, however, was the observation that, whereas pharmacological inhibition of dynamin and clathrin-mediated uptake had little effect on the uptake of the nonfunctionalized particles, these treatments resulted in a 70% reduction in the uptake of carboxylated NP. By contrast, inhibition of fluid-phase macropinocytosis uptake had the converse effect, leading the authors to conclude that the strong negative charge found in carboxylated NPs favored clathrin-mediated internalization. In addition to particle size and charge, shape and geometry are also probable determinants for the endocytosis mechanisms of a specific NP. Most uptake studies using quantitative fluorescence microscopy have focused on spherical particles; however, one study compared polystyrene spheres with elliptical disks [90]. In this work, particles ranged from 100 nm to 10 Mm in size, and were targeted to endothelial cells via intercellular adhesion molecule-1 (ICAM-1). Both geometries of particle were internalized through a mechanism involving actin, but the rate of internalization of the disks was significantly slower than that of spheres. These studies typically used pharmacological reagents in conjunction with semiquantitative fluorescence imaging to define internalization pathways taken by NPs. Although such an approach provides a basic understanding of the probable mechanisms used, it suffers from the problem that many of these chemical inhibitors lack specificity, and do not provide a means to assess systematically the molecular machinery with which internalized particles interact.

Following uptake, NPs are faced with a variety of intracellular pathways that they can take, involving multiple organelles. For most particle types, the default pathway following internalization is to lysosomes [91,92] Fluorescence-based imaging has made a major contributor to this observation, with many studies using colocalization of particles with fluorescent markers of lysosomes (e.g., LysoTracker®, or immunostaining with lysosomal proteins, such as LAMP1) [93,94]. Therefore, the spatial and temporal resolution offered by fluorescence microscopy provides quantitative data relating to the organelles through which NPs pass en route to the lysosomes. HCA has not yet been used to systematically study these intracellular trafficking pathways, although several recent quantitative microscopy studies suggest that this prospect is now realistic. One approach is to measure their colocalization with specific organelle markers. To this end, the Rab family of small GTP-binding proteins [95] is ideal, because there are approximately 60 members in human cells, each with a defined subcellular localization. In one such study in Caco-2 cells, polymeric NPs were exposed to cells for either 10 or 60 min and the cells were fixed and immunostained for Rab5 (early endosomes), Rab11 (recycling endosomes), and Rab7 (late endosomes/lysosomes). Analyses revealed a significant shift in colocalization strength from Rab5- to Rab7-positive membranes between the two time points, indicating the transfer of NPs from early endosomes to acidic (late) endosomes [96]. In a similar study, the same cell line was also used to study transcytosis of wheat germ agglutinin-functionalized NPs, although, on this occasion, the transient transfection of GFP fusions of endocytic Rabs, rather than antibodies, was used to define endosomal intermediates [97]. The transient expression of fluorescently labeled Rab proteins has also been used to define the endocytic profile of polystyrene NPs. Quantitative colocalization in live cells in three dimensions over 4 h was carried out, revealing that this particle type passed through Rab5-positive endosomes between 30 and 45 min after endocytosis, and that steady-state accumulation occurred in Rab7-positive structures within 120 min of uptake [98]. Such studies highlight that quantitative spatial and temporal analysis approaches are undoubtedly useful in defining the transport pathways taken by NPs inside cells and, therefore, we advocate further wide-ranging studies with greater use of automation as empowered by HCA.

Although most studies suggest that the preferred routing for a variety of NP types is to the lysosomes, understanding the extent to which particles can access other organelles, including the Golgi complex and endoplasmic reticulum, is also important [75]. Various fluorescence-based imaging studies suggest that a proportion, albeit often small, of certain types of particle can access early secretory pathway compartments. This is the case for NPs comprising PEI [99,100], DNA linked to PEG [101], and PLG [102], among others. Considering the variety of particle types available, and the diversity of intracellular destinations to which they could passage, it is logical to conclude that only high-throughput systematic approaches, such as HCA, will have the capacity to dissect this complexity. Furthermore, HCA lends itself well to being incorporated with methods such as RNAi that derive functional information about cellular processes and pathways. Small-scale RNAi studies have been used to quantify functionally the cell death pathways invoked by cationic NPs [103], and so a natural extension of this would be to use similar technology to quantitatively define uptake and trafficking mechanisms. As described above, image analysis strategies to date have typically used total cell-associated fluorescence and colocalization with organelle markers; however, HCA potentially provides a wider palette of quantification possibilities. It should be anticipated that these will be central to future systematic studies of particle uptake and trafficking.

Therefore, a more-focused strategy is to combine quantitative fluorescence microscopy with perturbations at an individual gene level through the use of RNAi. HCA in conjunction with genome-wide RNAi studies has already been used to evaluate the secretory pathway (Figure 8) [104] and the endocytotic pathway [105,106], and are powerful because HCA provides an unbiased and consistent quantification across all images and genes analyzed. To date, no such genome-wide characterization of NP uptake has been reported, but small-scale studies are now adding further depth to the pharmacological studies. For example, in the HCA study of the uptake of lipid NPs outlined above [81], siRNAs were used to deplete cells of fundamental endocytic machinery, and showed that lipid NPs primarily endocytose by either clathrin-mediation or macropinocytosis. The parallel study using a limited number of siRNAs also found that macropinocytosis (as judged by depletion of Cdc42 and Rac1) was important for the internalization of this particle type [82]. Thus, HCA, in combination with systematic RNAi, is likely to be a successful strategy to define more clearly at the molecular level the internalization mechanisms and intracellular trafficking pathways used by NPs.

Although HCA shows promise in the early-stage *in vitro* screening of particle delivery systems, there are current limitations to its application. HCA is more effective with adherent cells, whereas cells that do not exhibit contact inhibition growth are more complex to analyze. Similar to all forms of microscopy, care must be taken in the appropriate preparation and staining of samples for the endpoint being studied. To date, most studies have included HCA as an additional quantitative tool to traditional methods, validated by using biochemical assays. The true strength of this tool will only manifest when clear *in vitro–in vivo* correlations are seen for the current delivery technologies being screened. Previous *in vitro* tools have identified a range of promising particle delivery systems only for them to 'fail to deliver' at the preclinical or clinical stage of development. The importance of the data generated is also limited by the range of cell models available. A single cell type monoculture grown on a culture dish can not iteratively replicate the complex cellular mix and extracellular milieu of the body and the information derived on NP delivery is somewhat limited. Engineering of advanced co-cultures and tissue-engineered 3D constructs of various tissues is underway, but integrating these into a high-throughput environment is not trivial. Some of the most important information to be gleaned from these types of screen might be the information that can

be derived from subcellular trafficking studies that can elucidate the barriers to current intracellular delivery systems and inform design of future materials and platforms.

Concluding remarks

HCA is rapidly becoming the tool of choice in studying cell biology because of its high-throughput capacity for monitoring a range of morphometric, functional, and biochemical properties of cells. With the appropriate selection of cell model and use of nontoxic fluorescent dyes, cytotoxicity is easily detected at multiple levels. This technology is evolving with new hardware, new dyes, and user-friendly data analysis and is being applied for the assessment of the cytotoxicity of excipients and polymeric components of drug delivery systems, as well as for the uptake, intracellular trafficking, and cytotoxicity of NPs in a range of polarized and nonpolarized human cells. The power of this evolving tool is now an essential resource for multidisciplinary teams examining some of the most important research questions in cellular drug delivery.

Acknowledgments

This work was supported by the Science Foundation Ireland Centre for Medical Devices (CURAM), 13/RC/2073, the Irish Department of Agriculture FIRM grant (NUTRADEL), 11/F/042, and the European Union Seventh Framework Programme (FP7 / 2007-2013) under grant agreements n° 281035 ('TRANS-INT') and 310451 ('nanoMILE').

References

1 Medzihradsky, F. and Marks, M.J. (1975) Measures of viability in isolated cells. *Biochem. Med*. 13,164–177
2 Pappenheimer, A.M. (1917) Experimental studies upon lymphocytes. I. The reactions of lymphocytes under various experimental conditions. *J. Exp. Med*. 25,633–650
3 Weimar, V. (1962) Effect of amino acid, purine, and pyrimidine analogues on activation of corneal stromal cells to take up neutral red. *Invest. Opthamol*. 1,226–232
4 Porstmann, T. *et al.* (1985) Quantitation of 5-bromo-2–deoxyuridine incorporation into DNA: an enzyme immunoassay for the assessment of the lymphoid cell proliferative response. *J. Immunol. Methods* 82,169–179
5 Brunner, K.T. *et al. (*1968) Quantitative assay of the lytic action of immune lymphoid cells on ^{51}Cr-labelled allogeneic target cells *in vitro*; inhibition by isoantibody and by drugs. *Immunology* 14,181–196
6 Korzeniewski, C. and Callewaert, D.M. (1983) An enzyme-release assay for natural cytotoxicity. *J. Immunol. Methods* 64, 313–320
7 Mosmann, T. (1983) Rapid colorimetric assay for cellular growth and survival: application to proliferation and cytotoxicity assays. *J. Immunol. Methods* 65, 55–63
8 Berridge, M.V. *et al.* (1996) The biochemical and cellular basis of cell proliferation assays that use tetrazolium salts. *Biochemica* 96, 14–19
9 Page, B. *et al.* (1993) A new fluorometric assay for cytotoxicity measurements in vitro. *Int. J. Oncol.* 3, 473–476
10 Slaughter, M.R. *et al.* (1999) Evaluation of Alamar Blue reduction for the *in vitro* assay of hepatocyte toxicity. *Toxicol. In Vitro* 13, 567–569
11 Bernal, S.D. *et al.* (1982) Monitoring the effect of anti-cancer drugs on L1210 cells by a mitochondrial probe, rhodamine-123. *Int. J. Cancer* 30, 219–224
12 Brattin, W.J. *et al.* (1984) Assessment of the role of calcium ion in halocarbon hepatotoxicity. *Environ. Health Perspect.* 57, 321–323
13 O'Brien P.J. (2009) Discovery toxicology screening: predictive, *in vitro* cytotoxicity. In *Hit and Lead Profiling: Identification and Optimization of Drug-like Molecules* (Faller, B. and Urban, L., eds), pp: 325–344, John Wiley & Sons
14 Ragea, R. *et al.* (1990) DNA fluorometric assay in 96-well tissue culture plates using Hoechst 33258 after cell lysis by freezing in distilled water. *Anal. Biochem*. 191, 31–34
15 Skehan, P. *et al.* (1990) New colorimetric cytotoxicity assay for anticancer-drug screening. *J. Natl. Cancer Inst.* 82, 1107–1112
16 Crouch, SPM. *et al.* (1993) The use of ATP bioluminescence as a measure of cell proliferation and cytotoxicity. *J. Immunol. Methods* 160, 81–88
17 O'Brien, P.J. and Haskins, J.R. (2006) *In vitro* cytotoxicity assessment. *Methods Mol. Biol*. 356, 415–425
18 Bondesson, I. *et al.* (1989) MEIC – a new international multicenter project to evaluate the relevance to human toxicity of *in vitro* cytotoxicity tests. *Cell Biol. Toxicol*. 5, 331–347
19 Ekwall, B. (1999) Overview of the final MEIC results II. The *in vivo*/*in vitro* evaluation, including a selection of a practical battery of cell tests for prediction of acute lethal blood concentrations in humans. *Toxicol. In Vitro* 13, 665–73
20 Xu, J.J. *et al.* (2004) Applications of cytotoxicity assays and pre-lethal mechanistic assays for assessment of human hepatotoxicity potential. *Chem. Biol. Interact.* 150, 115–128
21 Schoonen, W.G. *et al.* (2005) Cytotoxic effects of 110 reference compounds on HepG2 cells and for 60 compounds on HeLa, ECC-1 and CHO cells. II Mechanistic assays on NAD(P)H, ATP and DNA contents. *Toxicol. in Vitro* 19, 491–503
22 Olson, H. *et al. (*2000) Concordance of the toxicity of pharmaceuticals in humans and in animals. *Regul. Toxicol. Pharmacol*. 32, 56–67
23 Segall, M.D. and Barber, C. (2014) Addressing toxicity risk when designing and selecting compounds in early drug discovery. *Drug Discov. Today* 19, 688–693
24 Diaz, D. *et al.* (2007) Evaluation of an automated *in vitro* micronucleus assay in CHOK1 cells. *Mutat. Res.* 630, 1–13
25 European Commission (2000) Test guideline B-41 phototoxicity: *in vitro* 3T3 NRU phototoxicity test of Annex V of the EU Directive86/906/EEC for classification and labelling of hazardous chemicals. *Off. J. Eur. Communities* L136, 98–107
26 O'Brien, P.J. *et al.* (2006) High concordance of drug-induced human hepatotoxicity with *in vitro* cytotoxicity measured in a novel cell-based model using high content screening. *Arch. Tox*. 80, 580–604
27 Abraham, V.C. (2008) Application of a high-content multiparameter cytotoxicity assay to prioritize compounds based on toxicity potential in humans. *J. Biomol. Screen*. 13, 527–537
28 Xu, J.J. *et al.* (2008) Cellular imaging predictions of clinical drug-induced liver injury. *Toxicol. Sci.* 105, 97–105
29 Tolosa, L. *et al.* (2012) Development of a multiparametric cell-based protocol to screen and classify the hepatotoxicity potential of drugs. *Toxicol. Sci.* 12, 127, 187–198
30 Garside, H. *et al.* (2014) Evaluation of the use of imaging parameters for the detection of compound-induced hepatotoxicity in 384-well cultures of HepG2 cells and cryopreserved primary human hepatocytes. *Toxicol. In Vitro* 28, 171–181
31 O'Brien, P.J. (2014) High content analysis in toxicology: screening substances for human toxicity potential, elucidating subcellular mechanisms, and *in vivo* use as translational safety biomarkers. *Basic Clin. Pharmacol. Toxicol.* 115, 4–17
32 Slaughter, M.R. *et al.* (2002) Effect of diquat on the antioxidant system and cell growth in human neuroblastoma cells. *Toxicol. Appl. Pharmacol.* 178, 63–70
33 Brayden, D.J. *et al.* (2014) A head-to-head multi-parametric high content analysis of a series of medium chain fatty acid intestinal permeation enhancers in Caco-2 cells. *Eur. J. Pharm. Biopharm*. 88, 830–839.
34 Rawlinson, L.B. *et al.* (2011) High content analysis of cytotoxic effects of pDMAEMA on human intestinal epithelial and monocyte cultures. *J. Control. Release* 146, 84–92

35 Iwai, R. *et al.* (2013) Enhanced transfection efficiency of poly(N,N-dimethylaminoethyl methacrylate)-based deposition transfection by combination with tris(hydroxymethyl)aminomethane. *Bioconjug Chem*. 24, 159–166

36 Green, J.B. *et al.* (2011) Antimicrobial testing for surface-immobilized agents with a surface-separated live-dead staining method. *Biotechnol Bioeng*. 108, 231–236

37 Paul, A. *et al.* (2014) Cytotoxicity mechanism of non-viral carriers polyethyleneimine and poly-L-Lysine using real time high content cellular assay. *Polymer* 55, 5178–5188

38 Maher, S. *et al.* (2014) Formulation strategies to improve oral peptide delivery. *Pharm. Pat. Anal.* 3, 313–336

39 Binkley, N. *et al.* (2012) A phase 3 trial of the efficacy and safety of oral recombinant calcitonin: the Oral Calcitonin in Postmenopausal Osteoporosis (ORACAL) trial. *J. Bone Miner. Res.* 27, 1821–1829

40 Tuvia, S. *et al.* (2014) A novel suspension formulation enhances intestinal absorption of macromolecules via transient and reversible transport mechanisms. *Pharm. Res.* 31, 2010–2021

41 Aungst, B. (2012) Absorption enhancers: applications and advances. *AAPS J.* 14, 10–18

42 Maher, S. *et al.* (2010) Impact of amino acid replacements on *in vitro* permeation enhancement and cytotoxicity of the intestinal absorption promoter, melittin. *Int. J. Pharm.* 387, 154–160

43 Walsh, E.G. *et al.* (2011) High content analysis to determine cytotoxicity of the antimicrobial peptide, melittin and selected structural analogues. *Peptides* 32, 1764–1773

44 Schellinger, J.G. *et al.* (2013) Melittin-grafted HPMA-oligolysine based copolymers for gene delivery. *Biomaterials* 34, 2318–2326

45 Soman, N.R. *et al.* (2009) Molecularly targeted nanocarriers deliver the cytolytic peptide melittin specifically to tumor cells in mice, reducing tumor growth. *J. Clin. Invest.* 119, 2830–2842

46 Mohan, H.M. *et al.* (2012) The mycotoxin, patulin, increases colonic epithelial permeability. *Food Chem. Toxicol.* 50, 4097–4102

47 Narkar, Y. *et al.* (2008) Evaluation of mucosal damage and recovery in the gastrointestinal tract of rats by a penetration enhancer. *Pharm. Res.* 25, 25–38

48 Wang, X. *et al.* (2010) Restoration of rat colonic epithelium after *in situ* intestinal instillation of the absorption promoter, sodium caprate. *Ther. Deliv.* 1, 65–72

49 Sakai, M. *et al.* (1998) Cytotoxicity of absorption enhancers in Caco-2 cell monolayers. *J. Pharm. Pharmacol.* 50, 1101–1108

50 Walsh, E. *et al.* (2011) Oral delivery of macromolecules: rationale underpinning Gastrointestinal Permeation Enhancement Technology (GIPET®). *Ther. Deliv.* 2, 1595–1610

51 Okuda, T. *et al.* (2006) Involvement of intracellular Ca2+ dynamics in cytoprotective action by amino acids and cytotoxicity by sodium laurate, an absorption enhancer. *J. Pharm. Sci.* 95, 2256–2265

52 Takayama, C. *et al.* (2009) Amino acids suppress apoptosis induced by sodium laurate, an absorption enhancer. *J. Pharm. Sci.* 98, 4629–4638

53 Walsh, E.G. *et al.* (2012) Misoprostol inhibits *in vitro* intestinal permeation enhancing effects of the medium chain fatty acid, sodium caprate (C_{10}) *Proc. Intern. Symp. Control. Rel. Bioact. Mater.* 39, Abstr. 687

54 Petersen, S.B. *et al.* (2012) Evaluation of alkyl maltosides as intestinal permeation enhancers: Comparison between rat intestinal mucosal sheets and Caco-2 monolayers. *Eur. J. Pharm. Sci.* 47, 701–712

55 Uchegbu, I.F. and Siew, A. (2013) Nanomedicines and nanodiagnostics come of age. *J. Pharm. Sci.* 102, 305–310

56 Tosi, G. *et al.* (2013).Potential use of polymeric nanoparticles for drug delivery across th blood-brain barrier. *Curr. Med. Chem.* 20, 2212–225

57 Bakhru, S.H. *et al.* (2013) Oral delivery of proteins by biodegradable nanoparticles. *Adv. Drug Deliv. Rev.* 65, 811–821

58 Rahman, M.A. *et al.* (2012) Systemic delivery of siRNA nanoparticles targeting RRM2 suppresses head and neck tumor growth. *J. Control. Release* 10, 384–392

59 Gaillard, P.J. *et al.* (2012) Enhanced brain delivery of liposomal methylprednisolone improved therapeutic efficacy in a model of neuroinflammation. *J. Control. Release* 164, 364–369

60 Salvati A. *et al.* (2013) Transferrin-functionalized nanoparticles lose their targeting capabilities when a biomolecule corona adsorbs on the surface. *Nat. Nanotechnol.* 8, 137–143

61 Mansour, H.M. *et al.* (2009) Nanomedicine in pulmonary delivery. *Int. J. Nanomedicine* 4, 299–319

62 Santo, V.E. *et al.* (2012) From nano- to macro-scale: nanotechnology approaches for spatially controlled delivery of bioactive factors for bone and cartilage engineering. *Nanomedicine* 7, 1045–1066

63 Kermanizadeh, A. *et al.* (2014) Toxicological effect of engineered nanomaterials on the liver. *Br. J. Pharmacol.* 171, 3980–3987

64 Zhang, T. *et al.* (2006) Cellular effect of high doses of silica-coated quantum dot profiled with high throughput gene expression analysis and high content cellomics measurements. *Nano. Lett.* 6, 800–808

65 Jan, E. *et al.* (2008) High-content screening as a universal tool for fingerprinting of cytotoxicity of nanoparticles. *ACS Nano.* 2, 928–938

66 Mironava, T. *et al.* (2010) Gold nanoparticles cellular toxicity and recovery: effect of size, concentration and exposure time. *Nanotoxicology* 4, 120–137

67 Joshi, H.M. *et al.* (2006) Gold nanoparticles as carriers for efficient transmucosal insulin delivery. *Langmuir* 22, 300–305

68 Patra, C.R. *et al.* (2010) Fabrication of gold nanoparticles for targeted therapy in pancreatic cancer. *Adv Drug Deliv Rev.* 62, 346–361

69 Khlebtsov, N. and Dykman, L. (2011) Biodistribution and toxicity of engineered gold nanoparticles: a review of *in vitro* and *in vivo* studies. *Chem. Soc. Rev.* 40,1647–1671

70 Byrne, S.J. *et al.* (2007) Jelly dots: synthesis and cytotoxicity studies of CdTe quantum dot-gelatin nanocomposites. *Small* 3, 1152–1156

71 Solmesky, L.J. *et al.* (2011) Assessing cellular toxicities in fibroblasts upon exposure to lipid-based nanoparticles: a high content analysis approach. *Nanotechnology* 22, 494016

72 Kedmi, R. *et al.* (2010) The systemic toxicity of positively charged lipid nanoparticles and the role of Toll-like receptor 4 in immune activation. *Biomaterials* 31, 6867–6875

73 Anguissola, S. *et al.* (2014) High content analysis provides mechanistic insights on the pathways of toxicity induced by amine-modified polystyrene nanoparticles. *PLoS ONE* 9, e108025

74 Nel, A.E. *et al.* (2009) Understanding biophysicochemical interactions at the nano-bio interface. *Nat. Mater.* 8, 543–557

75 Tarrago-Trani, M.T. and Storrie, B (2007) Alternate routes for drug delivery to the cell interior: pathways to the Golgi apparatus and endoplasmic reticulum. *Adv. Drug Deliv. Rev.* 59, 782–797

76 De Raad, M. *et al.* (2012) High-content screening of peptide-based non-viral gene delivery systems. *J. Control. Release* 158, 433–442

77 Deng, Y. *et al.* (2014) Therapeutic potentials of gene silencing by RNA interference: principles, challenges, and new strategies. *Gene* 538, 217–227

78 McKiernan, P.J. *et al.* (2013).Targeting miRNA-based medicines to cystic fibrosis airway epithelial cells using nanotechnology. *Int. J. Nanomedicine* 8, 3907–3915

79 Lawlor, C. *et al.* (2011) The application of high-content analysis in the study of targeted particulate delivery systems for intracellular drug delivery to alveolar macrophages. *Mol. Pharm.* 8, 1100–1112

80 Kelly, C. *et al.* (2014) Therapeutic aerosol bioengineering of siRNA for the treatment of inflammatory lung disease by TNFα gene silencing in macrophages. *Mol Pharm.* 11, 4270–4279.
81 Gilleron, J. *et al.* (2013) Image-based analysis of lipid nanoparticle-mediated siRNA delivery, intracellular trafficking and endosomal escape. *Nat. Biotechnol.* 31, 638–646
82 Sahay, G. *et al.* (2013) Efficiency of siRNA delivery by lipid nanoparticles is limited by endocytic recycling. *Nat. Biotechnol.* 31, 653–658
83 Kelly, C. *et al.* (2014) High throughput methods for screening liposome–immune macrophage cell interaction. *J. Liposome Res.* 30, 1–11
84 Manchian, B.B. *et al.* (2014) High-content imaging and gene expression analysis to study cell-nanomaterial interactions: the effect of surface hydrophobicity. *Biomaterials* 5, 9941–9500
85 Algahtani, M.S. *et al.* (2014) High throughput screening for biomaterials discovery. *J. Control. Release* 190, 115–126
86 Rejman, J. *et al.* (2004) Size-dependent internalization of particles via the pathways of clathrin- and caveolae-mediated endocytosis. *Biochem. J.* 377(Pt 1), 159–169
87 Lühmann, T. *et al.* (2008) Cellular uptake and intracellular pathways of PLL-g-PEG-DNA nanoparticles. *Bioconjug. Chem.* 19, 1907–1916
88 Liu, P. *et al.* (2014) Intracellular trafficking and cellular uptake mechanism of mPEG-PLGA-PLL and mPEG-PLGA-PLL-Gal nanoparticles for targeted delivery to hepatomas. *Biomaterials* 35, 760–770
89 Jiang, X. *et al.* (2011) Specific effects of surface carboxyl groups on anionic polystyrene particles in their interactions with mesenchymal stem cells. *Nanoscale* 3, 2028–2035
90 Muro, S. *et al.* (2008) Control of endothelial targeting and intracellular delivery of therapeutic enzymes by modulating the size and shape of ICAM-1-targeted carriers. *Mol. Ther.* 16, 1450–1458
91 Sahay, G. *et al.* (2010) Endocytosis of nanomedicines. *J. Control. Release* 145, 182–195
92 Treuel, L. *et al.* (2013) New views on cellular uptake and trafficking of manufactured nanoparticles. *J. R. Soc. Interface* 10, 20120939
93 Contreras, J. *et al.* (2010) Intracellular uptake and trafficking of difluoroboron dibenzoylmethane-polylactide nanoparticles in HeLa cells. *ACS Nano.* 4, 2735–2747
94 Wang, F. *et al.* (2013) Time resolved study of cell death mechanisms induced by amine-modified polystyrene nanoparticles. *Nanoscale* 5, 10868–10876
95 Stenmark, H. (2009) Rab GTPases as coordinators of vesicle traffic. *Nat. Rev. Mol. Cell Biol.* 10, 513–525
96 He, B. *et al.* (2013) The transport mechanisms of polymer nanoparticles in Caco-2 epithelial cells. *Biomaterials* 34, 6082–6098
97 Song, Q. *et al.* (2012) Mechanisms of transcellular transport of wheat germ agglutinin-functionalized polymeric nanoparticles in Caco-2 cells. *Biomaterials* 33, 6769–6782
98 Sandin, P. *et al.* (2012) High-speed imaging of Rab family small GTPases reveals rare events in nanoparticle trafficking in living cells. *ACS Nano.* 6, 1513–1521
99 Reilly, M.J. *et al.* (2012) Polyplexes traffic through caveolae to the Golgi and endoplasmic reticulum en route to the nucleus. *Mol. Pharm.* 9, 1280–1290
100 Fichter, K.M. *et al.* (2013) Polymeric nucleic acid vehicles exploit active interorganelle trafficking mechanisms. *ACS Nano.* 7, 347–364
101 Kim, A.J. *et al.* (2011) Non-degradative intracellular trafficking of highly compacted polymeric DNA nanoparticles. *J. Control. Release* 158, 102–107
102 Cartiera, M.S. *et al.* (2009) The uptake and intracellular fate of PLGA nanoparticles in epithelial cells. *Biomaterials* 30, 2790–2798
103 Bexiga, M.G. *et al.* (2013) RNA interference-mediated inhibition of apoptosis fails to prevent cationic nanoparticle-induced cell death in cultured cells. *Nanomedicine* 9, 1651–1664.
104 Simpson, J.C. *et al.* (2012) Genome-wide RNAi screening identifies human proteins with a function in the early secretory pathway. *Nat. Cell Biol.* 14, 764–774
105 Collinet, C. *et al.* (2010) Systems survey of endocytosis by multiparametric image analysis. *Nature* 464, 243–249
106 Liberali, P. *et al.* (2014) A hierarchical map of regulatory genetic interactions in membrane trafficking. *Cell* 157, 1473–1487

Figure 1. [LM5]Instrumentation exploits high-throughput multiwell automation with epifluorescence microscopy and multi-wavelength fluorescent dye analysis. Following 24-h initial incubation in 96-well plates, cells are exposed to agent for set periods and stained with dye cocktail to mark parameters. The plate is docked in the live cell chamber at 37ºC for analysis. Images are acquired at 10× or 20× magnification and are subjected to segmentation analysis, yielding quantitative data for both individual cells and cell populations; these are used in tandem with the fluorescent micrographs taken during acquisition. Adapted, with permission, from [43].

Figure 2. High-content analysis (HCA) assay reveals drug-induced cytotoxicity. **(A)** Untreated HepG2 cells. **(B)** HepG2 treated with 100-MM fluvastatin for 3 days. **(C)** Untreated Jurkat cells. **(D)** Jurkat lymphocytes treated with 0.2-MM mitoxantrone for 3 days. Healthy cells have blue-stained nuclei and red-stained mitochondria. Cytotoxic cells lose their mitochondrial activity, have an increased concentration of calcium, stained green, and increased membrane permeability resulting in a red dye diffusing to the nucleus. Scale bar = 18 μm (A, B); 15 μm (C,D). P.J. O'Brien, unpublished data[LM6].

Figure 3. Title[LM7]. **(A)** Concentration–response curves of effects of poly(2-(dimethylamino ethyl)methacrylate) (pDMAEMA) on Caco-2 and U937 cells after 72-h exposure. Readings were compared with 100% negative controls. * P <0.05, ** P <0.01, *** P <0.001 compared with controls containing no drug. pDMAEMA had no effect on phospholipidosis in **(B)** U937 cells and **(C)** Caco-2 cells. Black squares = 24 h, black triangles = 48 h, white squares = 72 h. * P <0.05, ** P <0.01, *** P <0.001 compared with 100% controls containing no drug. Positive control: erythromycin (Ery, 250 μg/ml); Triton X-100 (TTX, 0.01%). Reproduced, with permission, from [34]. Abbreviations: CN, cell number; MMP, mitochondrial membrane potential; NA, nuclear area; NI, nuclear intensity; PMP, plasma membrane potential.

Figure 4. Title[LM8]. **(A)** There is a strict inverse correlation for medium-chain fatty acid (MCFA) carbon chain length (C_8–C_{12}) and the concentrations required to increase the apparent permeability coefficient for [^{14}C]-mannitol across filter-grown Caco-2 monolayers detoxed at 120 min. Changes in intracellular calcium (IC) and plasma membrane permeability (PMP) determined with high-content analysis (HCA) in Caco-2 cells in 96-well filters following 60-min exposure tightly correlate with chain length and apparent permeability coefficient (Papp). **(B)** Representative HCA images of Caco-2 cells after 60-min exposure to C_{10}. (i) Untreated; (ii) 5 mM; (iii) 8.5 mM. Each fused fluorescent image was acquired at 20× objective magnification and pseudo-colored accordingly; Hoechst® (nuclear staining; blue), Fluo-4 AM (green; measure of IC), TOTO®-3 iodine (magenta; measure of PMP) and tetra-methyl rhodamine (TMRM; red; measure of mitochondrial membrane potential, MMP). Scale bar = 20 μm. **(C)** Data derived support a model of surfactant hydrophobic group insertion into bilayers to cause intestinal epithelial membrane fluidization and subsequent permeability increases. Reproduced, with permission, from [33] (A,B).

Figure 5. Exposure to polystyrene particles: high-content analysis (HCA) reveals cytotoxicity of aminated 50-nm nanoparticles (NPs; PS-NH_2) compared with plain (PS Plain) or carboxylated NP (PS-COOH). Seven cell lines were exposed to vehicle (ctrl) or increasing concentrations of NPs for 24 h, of which data from two lines are shown here. The lines were assessed based on changes in nuclear morphology (Hoechst), mitochondrial membrane potential [tetra-methyl rhodamine (TMRM)], cytosolic calcium levels (Fluo-4), lysosomal acidification (Lysotracker green), and plasma membrane integrity (TOPRO-3.; The graphs show for both cell lines and each parameter the concentration-dependent changes caused by PS-NH_2 NPs (continuous line) whereas PS-COOH NPs did not cause any effect (dashed line). Concentration responses for PS-Plain NPs are not shown, because they overlapped with the PS-COOH responses. Data are shown as average ± standard deviation (SD) of 45 acquired images from three independent experiments. The y-axis is arbitrary fluorescent units. Adapted, with permission, from [73], with minor modifications to the legend.

Figure 6. High-content analysis (HCA) of miRNA-Dy547-loaded nanoparticles (NPs) associated with cystic fibrosis transmembrane conductance regulator bronchial epithelial (CFBE)41o- cells at 20-h post transfection. **(A)** Comparative quantification of fluorescent miRNA delivered to CFBE cells by polyethyleneimine (PEI)- and chitosan-based NPs at different nitrogen:phosphorous (N/P) ratios and compared with the commercial transfection agent, RiboJuice™. Data are represented as mean fluorescence intensity normalized to relative carrier [i.e., PEI, chitosan or chitosan- tripolyphosphate (TPP) uncomplexed] ± standard error of the mean and were compared by one-way analysis of variance followed by Bonferroni's multiple comparison test. Differences were considered significant at P ≤0.05. ***P ≤0.001. **(B)**

Images of miRNA nanoparticles (red) associated with CFBE cells (blue, nucleus; green, F-actin; arrow, area shown in higher zoom box). Reproduced, with permission, from [78].

Figure 7. [LM9]High-content analysis (HCA) of small interfering (si)RNA–microparticle interaction with primary macrophages. Human monocytes were isolated and allowed to adhere to 96-well plates. Cells were transfected with empty microparticles (MP) or fluorescently tagged (fl) siRNA alone (AlexaFluor 488, green), or encapsulated in microparticles (siRNA-MP). Following 2 or 24 h incubation, cells were fixed and counterstained with phalloidin-TRITC (F-actin, red) and Hoechst (nucleus, blue). Images were acquired at 10× using an InCell® 1000 showing **(A)** untreated cells and **(B)** cells treated with 100 mg Fl-siRNA-MPs; **(C)** the number of fl-siRNA particles was counted per cell using InCell® 1000. Data are represented as mean ± standard deviation (SD) (n = 3). Statistical significance was determined by two-way analysis of variance followed by Bonferroni post-hoc test (*p <0.05) versus empty microparticle counterparts. Reproduced, with permission, from [80].

Figure 8. [LM10]High-content analysis (HCA) options for analyzing nanoparticle (NP) uptake and distribution in cultured cells. The example shows possible HCA approaches for NP analysis in cells. Raw images showing NPs (red) inside cells with nuclei labeled (blue) are subjected to HCA, specifically enabling the segmentation of cell boundaries, cell nuclei, and the NPs themselves. For accurate analysis, NP must be correctly assigned to individual cells (color coded). This step also enables cells on the border of the image to be discounted from subsequent analysis. Following segmentation, a range of measurement and analysis possibilities are available. These include simple measurement of NP intensity and number per cell; quantitative colocalization with organelle-specific markers (assuming another color channel was acquired); time-lapse information (if images were acquired from live cells over time); and texture analysis (e.g., spot-edge-ridge features) to provide complex information on NP density and distribution in the cells.

Table 1. HCA modern cytotoxicity assays versus traditional assays[a]

Parameter	HCA	Traditional assays
Data from entire population	Dissects different responses in different cells	Averages out data that might result in at least partial cancellation of responses
Single cell microscopy	Fluorescence imaging delineates cells	Limited
Subcellular organelle detail	Fluorescence imaging of specific organelle changes or biomarker translocation	No
Spatial resolution	Yes	No
Temporal resolution	Parameters can be monitored every second	No
Sublethal mechanistic data	Initiating data and sequential pathophysiological changes define mechanism	No, typically viability or single endpoint
Multiparametric monitoring	Four functional and multiple morphometric parameters that are measureable simultaneously and without interactions	Single-parameter assays
Live-cell, real-time, iterative, kinetic monitoring	Individual live cells are monitored continuously in real time	Single endpoint measures on dead cells; cannot be repeated
Adapted for acute and chronic exposure	Incubation for up to 72 h in selected cells as appropriate for expression of toxicity	Tend to be acute exposure assays with no basis for timings
Automated	Fully automated from time of putting plate on; algorithms available for data analysis	No
Rapid throughput	Yes, suitable for robotics given origin in discovery	Labor intensive
Metabolism-dependent cytotoxicity	Metabolite-mediated toxicity requires cells expressing xenobiotic metabolic competence	Same issue
Receptor-dependent cytotoxicity	Receptor-mediated toxicity requires choice of cells expressing appropriate target receptor	Same issue
Full dose–response relation	Automated rapid throughput determines full concentration–response relation and hormesis	Usually not practical
Relation to therapeutic index	Data are relevant because are multiples of effective concentration of compound	Same issue
Translational from *in vitro* to *in vivo*	Demonstrated to be applicable *in vivo*	Only demonstrated *in vitro*
Applicable to most cytotoxicities	Adapted to a range of cell types, organelles, and physiological processes	Variation in methodological and technological approaches

[a]Based on [31].

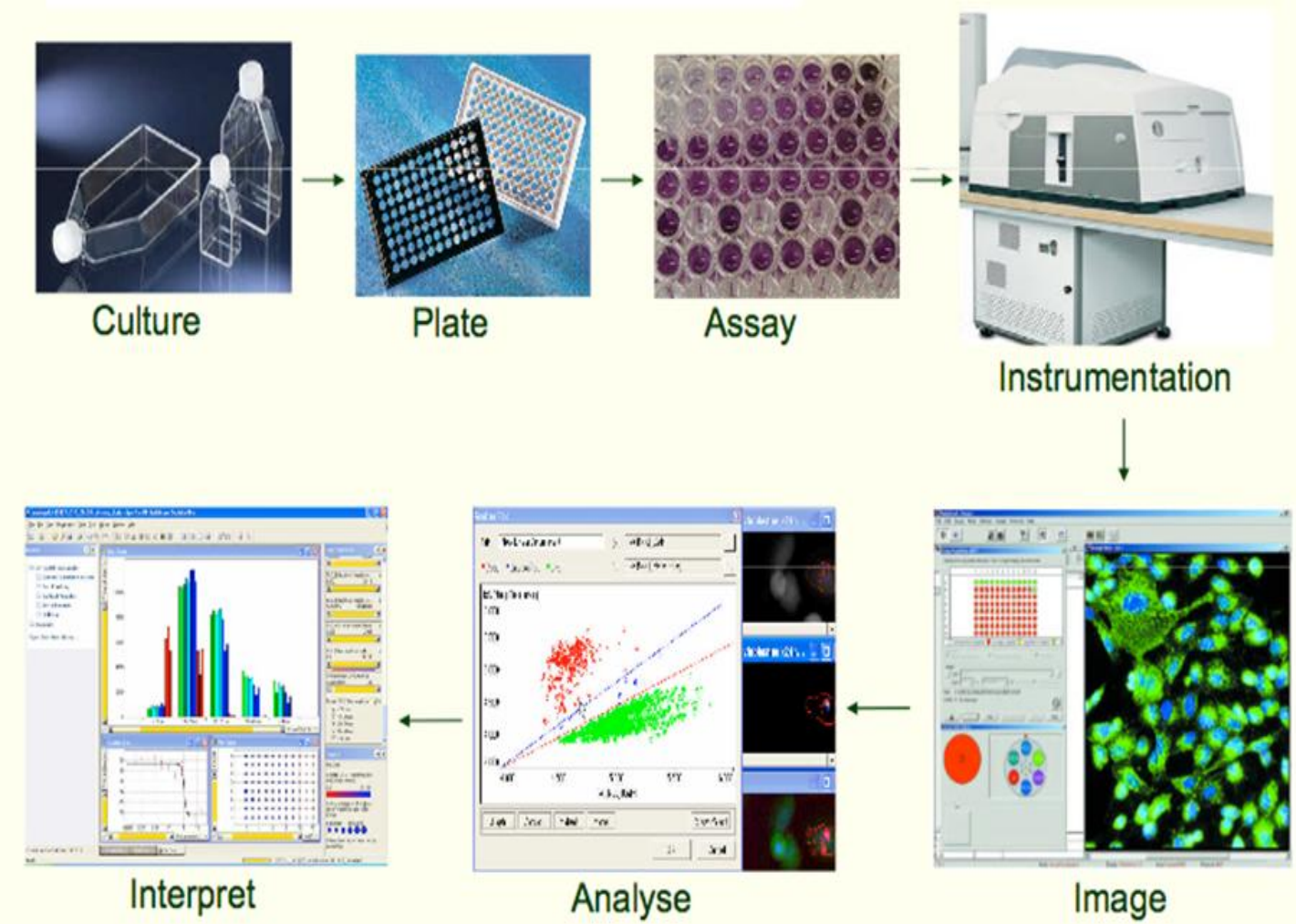
Culture
Plate
Assay
Instrumentation
Image
Analyse
Interpret

Fig. 1

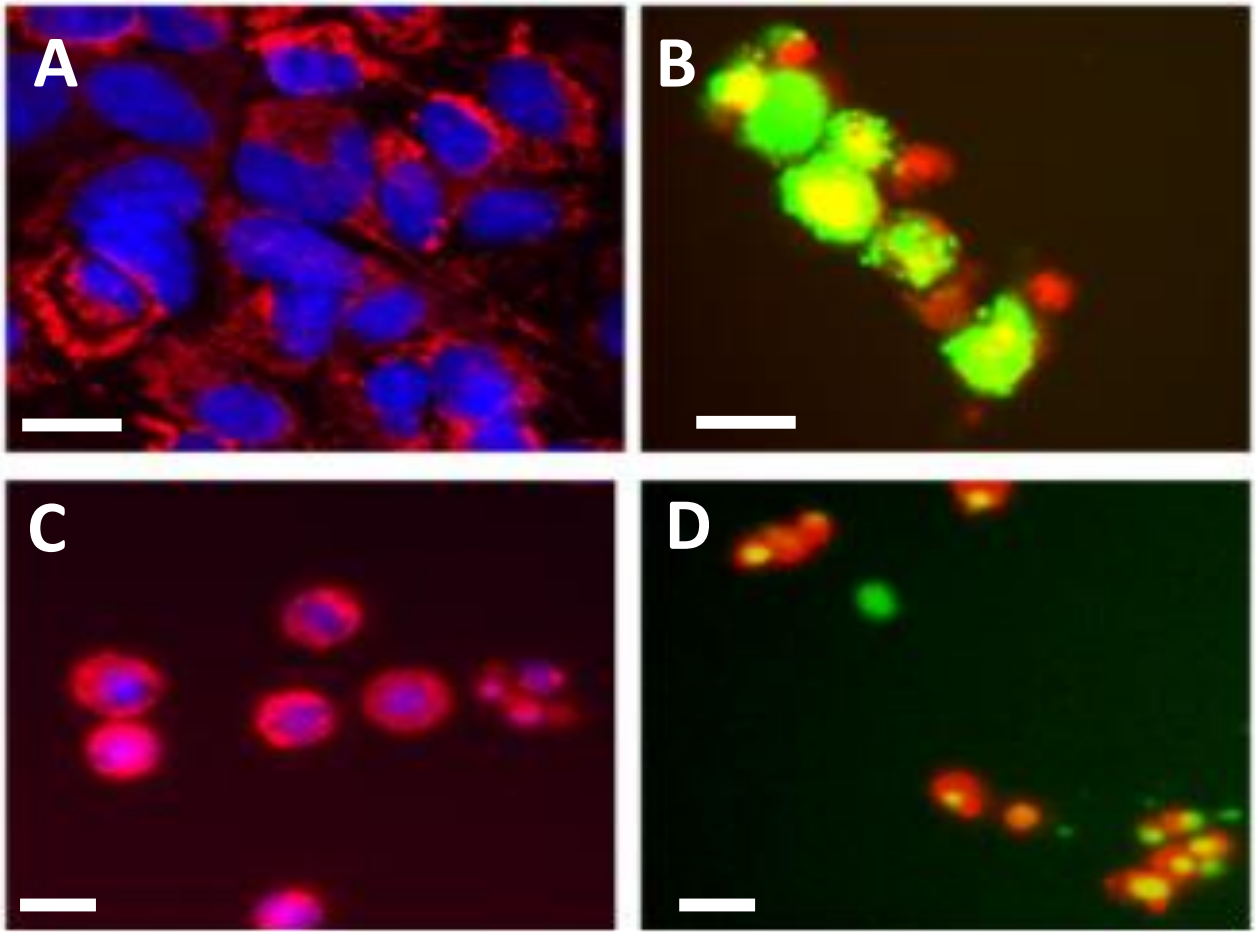

Fig. 2

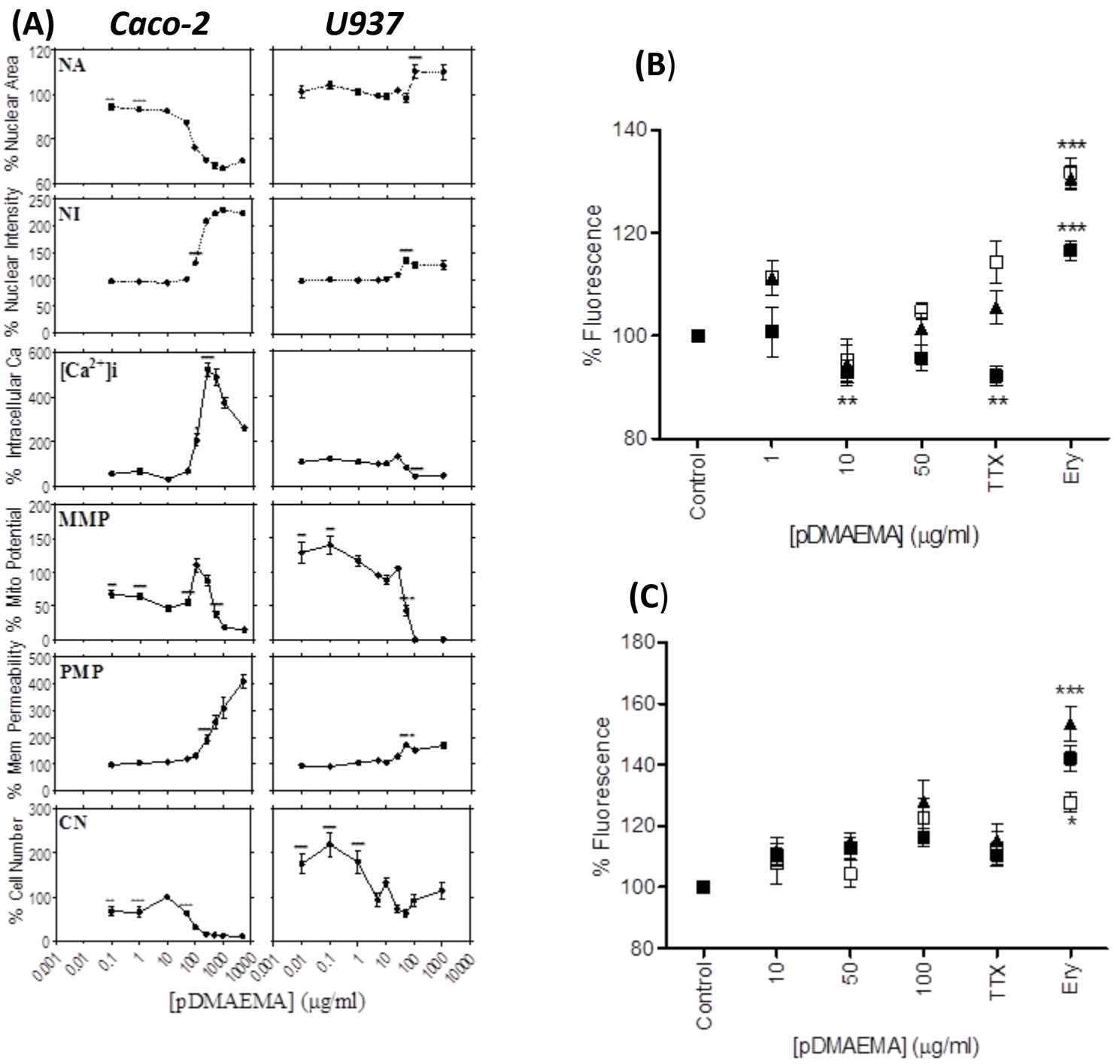
(A)
Caco-2
U937
NA
% Nuclear Area
NI
% Nuclear Intensity
[Ca2+]i
% Intracellular Ca
MMP
% Mito Potential
PMP
% Mem Permeability
CN
% Cell Number
0.001
0.01
0.1
1
10
100
1000
10000
[pDMAEMA] (µg/ml)
(B)
% Fluorescence
Control
1
10
50
TTX
Ery
[pDMAEMA] (µg/ml)
(C)
% Fluorescence
Control
10
50
100
TTX
Ery
[pDMAEMA] (µg/ml)

Fig 3

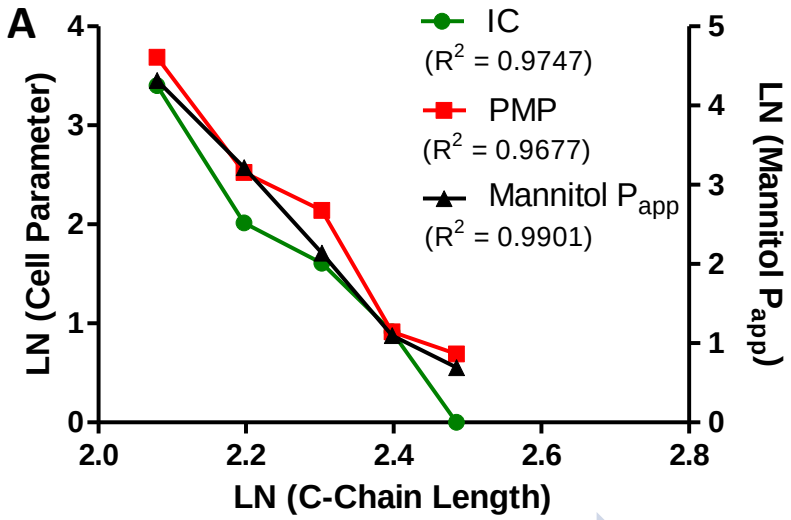
A
IC
(R^2 = 0.9747)
PMP
(R^2 = 0.9677)
Mannitol P_{app}
(R^2 = 0.9901)
LN (Cell Parameter)
LN (Mannitol P_{app})
LN (C-Chain Length)
0
1
2
3
4
5
2.0
2.2
2.4
2.6
2.8

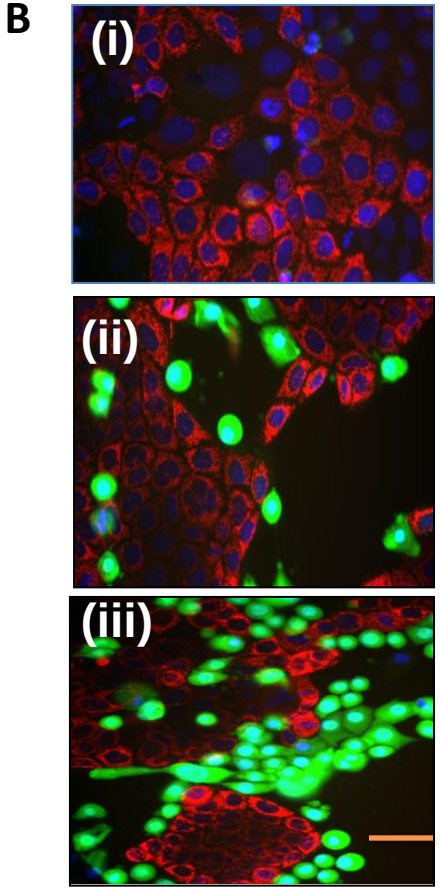
B
(i)
(ii)
(iii)

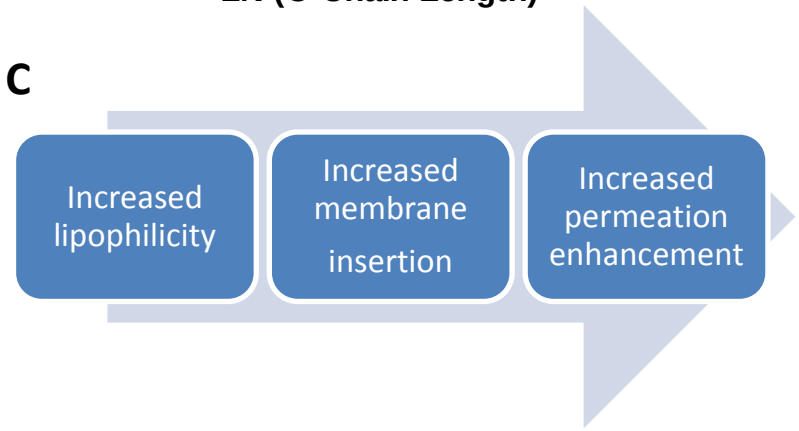
C
Increased lipophilicity
Increased membrane insertion
Increased permeation enhancement

Fig. 4

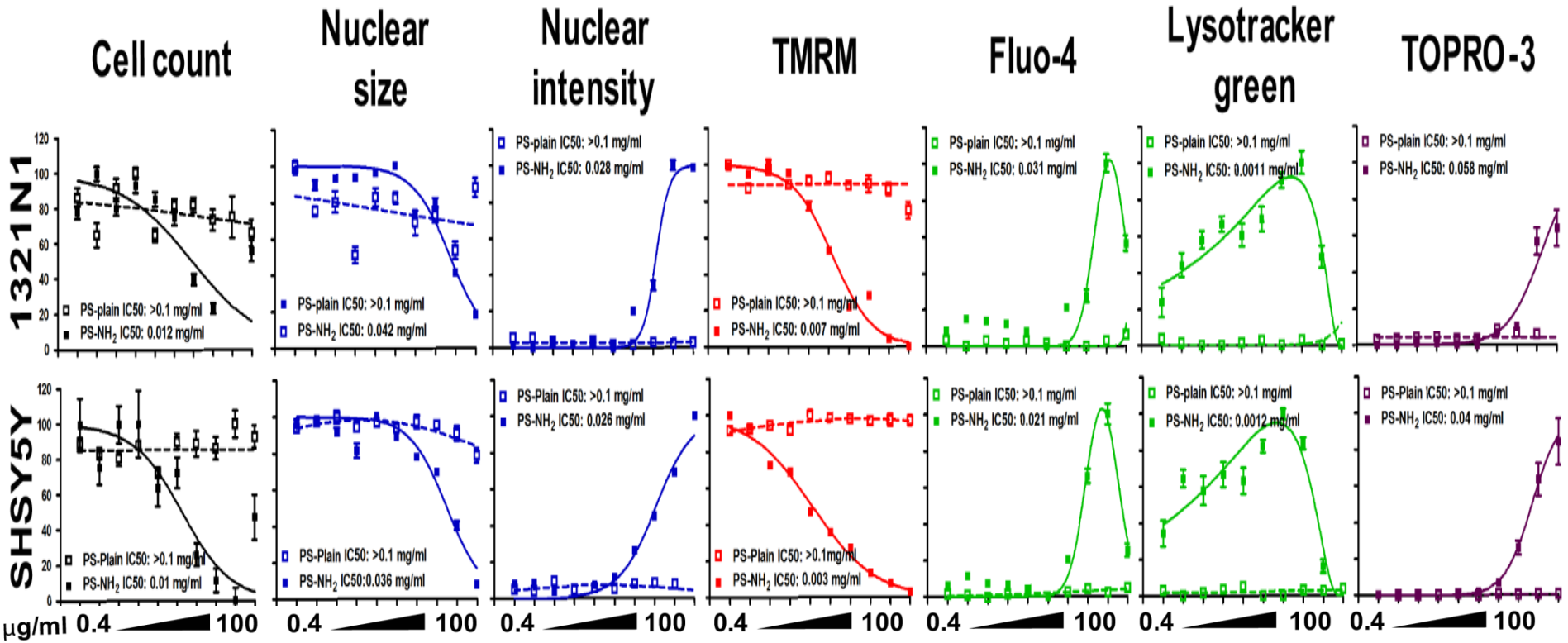
Cell count
Nuclear size
Nuclear intensity
TMRM
Fluo-4
Lysotracker green
TOPRO-3
1321N1
SHSY5Y
PS-plain IC50: >0.1 mg/ml
PS-NH2 IC50: 0.012 mg/ml
PS-plain IC50: >0.1 mg/ml
PS-NH2 IC50: 0.042 mg/ml
PS-plain IC50: >0.1 mg/ml
PS-NH2 IC50: 0.028 mg/ml
PS-plain IC50: >0.1 mg/ml
PS-NH2 IC50: 0.007 mg/ml
PS-plain IC50: >0.1 mg/ml
PS-NH2 IC50: 0.031 mg/ml
PS-plain IC50: >0.1 mg/ml
PS-NH2 IC50: 0.0011 mg/ml
PS-plain IC50: >0.1 mg/ml
PS-NH2 IC50: 0.058 mg/ml
PS-Plain IC50: >0.1 mg/ml
PS-NH2 IC50: 0.01 mg/ml
PS-Plain IC50: >0.1 mg/ml
PS-NH2 IC50:0.036 mg/ml
PS-Plain IC50: >0.1 mg/ml
PS-NH2 IC50: 0.026 mg/ml
PS-Plain IC50: >0.1mg/ml
PS-NH2 IC50: 0.003 mg/ml
PS-plain IC50: >0.1 mg/ml
PS-NH2 IC50: 0.021 mg/ml
PS-plain IC50: >0.1 mg/ml
PS-NH2 IC50: 0.0012 mg/ml
PS-Plain IC50: >0.1 mg/ml
PS-NH2 IC50: 0.04 mg/ml
µg/ml 0.4 100
0.4 100
0.4 100
0.4 100
0.4 100
0.4 100
0.4 100

Fig. 5

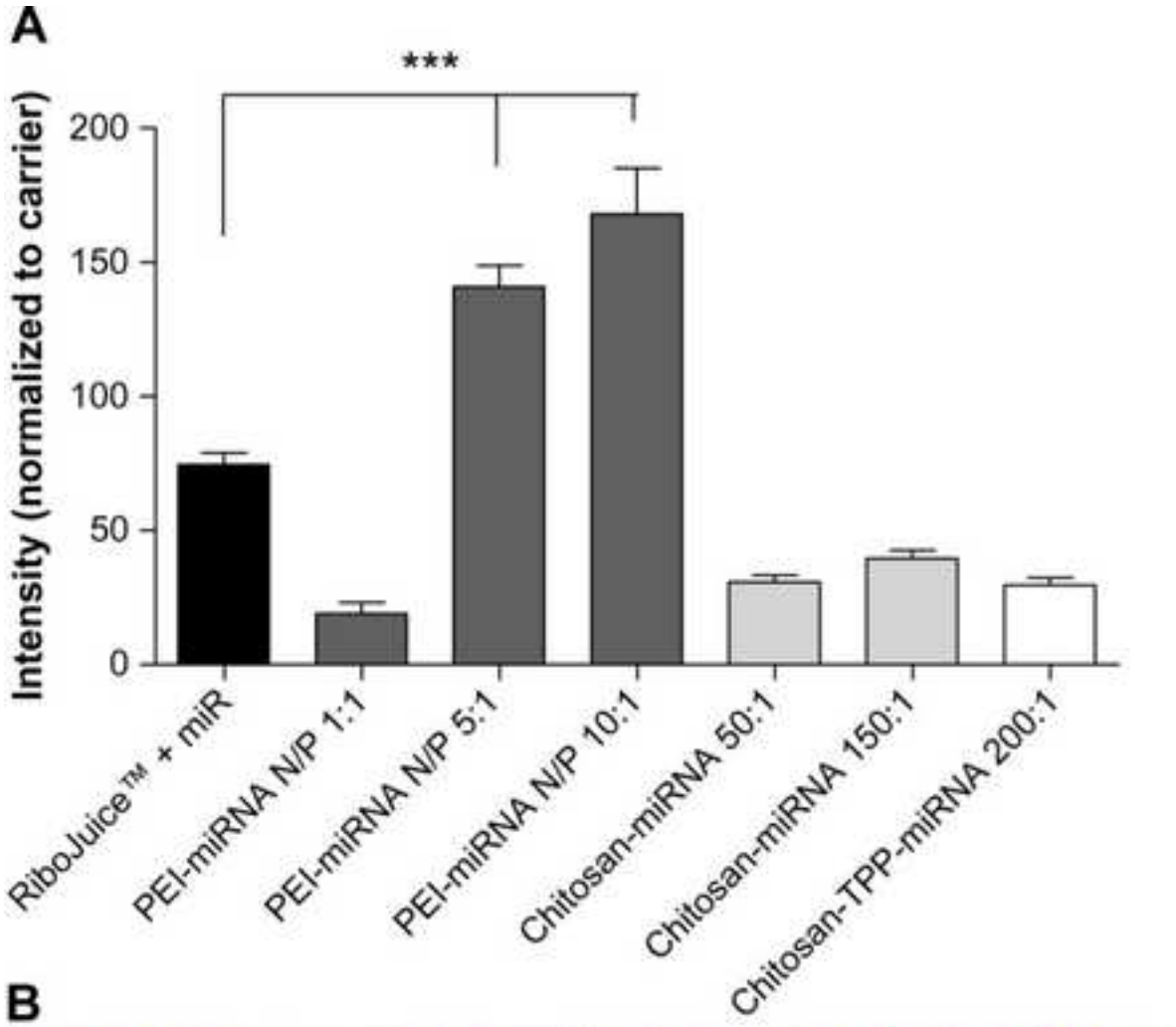

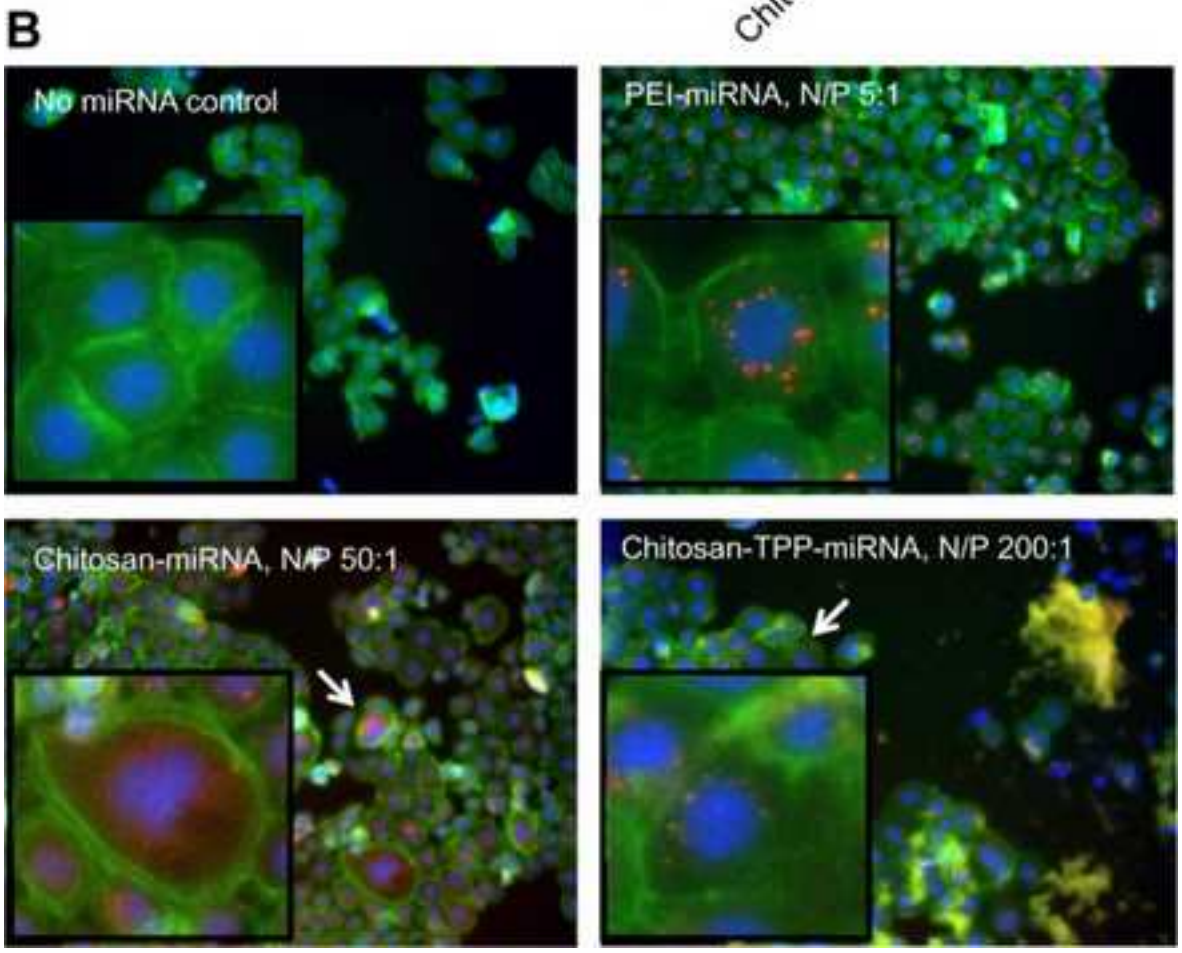

Figure 7

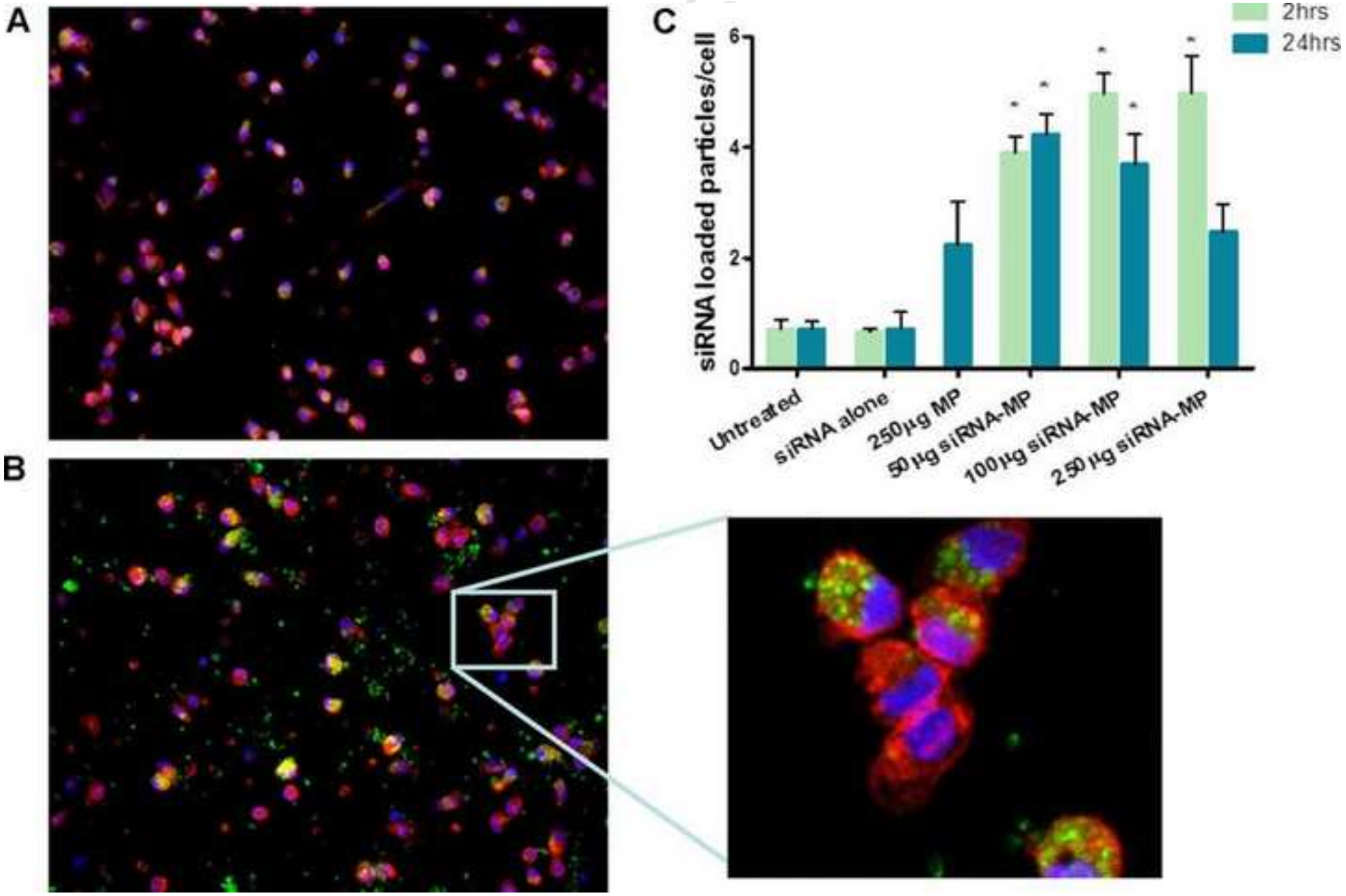
A
B
C
2hrs
24hrs
siRNA loaded particles/cell
0
2
4
6
Untreated
siRNA alone
250µg MP
50 µg siRNA-MP
100µg siRNA-MP
250 µg siRNA-MP

Figure 8

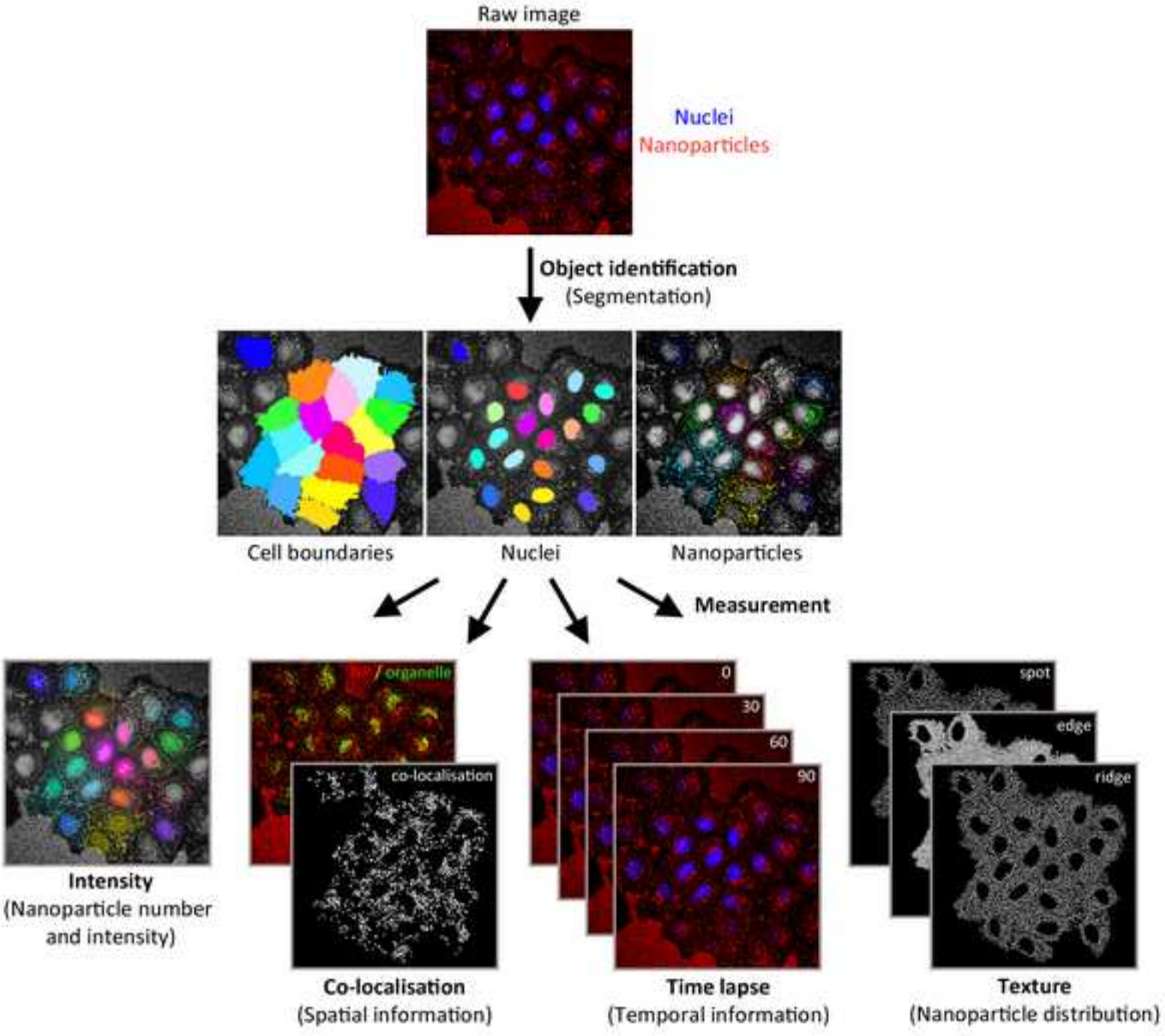
Raw image
Nuclei
Nanoparticles
Object identification
(Segmentation)
Cell boundaries
Nuclei
Nanoparticles
Measurement
Intensity
(Nanoparticle number and intensity)
organelle
co-localisation
Co-localisation
(Spatial information)
0
30
60
90
Time lapse
(Temporal information)
spot
edge
ridge
Texture
(Nanoparticle distribution)

Author Photo 2 Cryan

Graphical Abstract (for review)